UNIVERSITY OF BIRMINGHAM

The Effects of Acrylic Acid On The Electro-Mechanical Behaviour of ITO-Coated Polymer Substrates for Flexible Display Technologies

By

Kyle Burrows

A thesis submitted to

The University of Birmingham

For the degree of

MASTER OF RESEARCH

School of Metallurgy and Materials

The University of Birmingham

September 2012

Abstract

The effects of acrylic acid on the electro-mechanical behaviour of commercial ITO/PET systems for use in thin flexible displays were investigated under uniaxial tension and monotonic bending under both tensile and compressive stresses of the ITO coated surface within the ITO/PET system. The tribological properties of these systems were also investigated using a fretting technique under dry sliding conditions via a customised High Frequency Reciprocating Rig. Changes in electrical resistance were monitored *in situ*. *Ex situ* SEM was conducted to provide surface characterisation of the mechanically-tested samples. The results showed when tested under tension the ITO/PET systems ability to resist strain was significantly reduced in both uniaxial tensile testing and monotonic bending after exposure to acrylic acid. The main failure mechanism is suggested to be stress-corrosion cracking. However when tested in compression, the exposure to acrylic acid was not seen to have an effect on the electro-mechanical properties. The tribological properties of these thin film systems were also seen to be affected by the exposure to acrylic acid as; the number of cycles to failure for the 300 Ω/□ sample was reduced from 570 cycles to 200 cycles.

“Did you hear about the rose that grew

from a crack in the concrete?

Proving nature's law is wrong it

learned to walk without having feet.

Funny it seems, but by keeping its dreams,

it learned to breathe fresh air.

Long live the rose that grew from concrete

when no one else ever cared”

T. Shakur

Acknowledgements

I would like to thank my supervisor Dr Stephen Kukureka and fellow colleague Grzegorz Potoczny for their academic support and guidance throughout this project. I would also like to thank Mr Frank Biddlestone for all his technical support in the laboratory.

A special thank you needs to be given to Dr Karl Dearn, Jakub Piaszyk, Andrew Hoover and Dr Darran Cairns for their help and support in developing customisations to the High Frequency Reciprocating Rig.

Finally I would like to thank my family and most importantly, I would like to thank my mother for all her love, help and support.

Contents

1. Introduction

1.1 Introduction to displays

We often take them for granted, however displays are present in every aspect of our modern day life; they are present in the forms of televisions, personal computers and mobile phones to name only a few. Displays have constant impact on our lives and consumers are becoming familiar with new technologies and are also pushing for new innovations. The evolution of display technology has rapidly grown over the past decade, the cathode ray tube (CRT) display screens that once dominated the market are now archaic and the thin liquid crystal display matrix (LCD) technologies that surpassed them are now over 30 years old. Innovation has now moved into the possibility of manufacturing flat, flexible displays. However for the manufacturing process to be viable, flat flexible substrates must be found to replace the conventional glass substrates currently used. Displays have always been a pinnacle aspect to the consumer, as they are the interface between us humans and machines.

1.1.2 Touch screen applications

Touch screens have become very popular in mobile devices as they are aesthetically pleasing; save space by combining the display and input area, allow dynamic simulation of electro-mechanical controls such as buttons and engage the user in simple, effortless control at their finger tips. Touch screen panels are manufactured with multiple layers. The top layer consists of a polymer film whilst the bottom layer is manufactured from glass which acts as a sensor (Sierros, 2006). Both of these layers are coated with TCO's (Transparent Conducting Oxides) such as Indium Tin Oxide. These layers are separated by a middle layer of dielectric spacers. The interface functions when an electrical current is applied to the polymer layer and

a finger compresses the top film layer. The polymer film then comes into contact with the bottom layer glass sensor and a controller detects the current flow to the corners of the display panel and with this information it is able to calculate and detect the geometry of the finger on the display (Crawford, 2000)

1.1.3 Flexible displays

The evolution of the display industry is rapidly growing year on year, with a gained interest into the topic of flexible display technology. Slikkerveer (2002) defined a flexible display as; "A flat panel display constructed of thin (flexible) substrates that can be bent, flexed, conformed, or rolled to a radius of curvature of a few centimetres without losing functionality". With regards to the requirements of the display to be bent to a radius of curvature whilst still maintaining key functional properties, a flexible display can be further classified into *formed* and *flexible* via the degree of flexibility it will see in service. *Formed* displays are bent once to a specified radius of curvature, and are ideal for the automotive industry such as a display that fits right inside the dashboard. Unlike a formed display which is flexed once and no further, a *flexible* display may be bent and flexed multiple times during use.

The future developments for flexible display technologies are promising, however their introduction to the consumer market is still dependant on technical and manufacturing developments. In terms of a substrate material that conforms to the previously stated design parameters that define a flat flexible display, Polymers offer a number of advantages. Polymers are light weight, conformable, transparent and most of all flexible. In comparison to the rigid mechanical properties of the traditional glass substrates that are currently used in flat panel television display technology such as the liquid crystal displays, which makes it

more than difficult to manufacture into a flexible display substrate, the mechanical properties of polymers can range from engineering polymers of high rigidity to soft rubbers and films. Moreover they offer the advantage of enabling a higher profit margin in the consumer market due to their combination of low base value and suitability to be mass produced by a viable roll to roll manufacturing process. This in turn has developed into the development of research for polymer use not only in the television display industry, but they are being considered as a key substrate material in a range of applications including; organic light emitting diodes (OLED's), dielectric materials and transparent substrates (Choi et al., 2008).

However the service efficiency and lifetime of these flexible displays is heavily dependent on the polymers mechanical, electrical and optical properties. Therefore it is essential that care is taken when choosing the correct polymer to be used as a flexible substrate as many do not fulfil the reliability requirements of display processing as they may exhibit poor mechanical, structural and/or chemical properties (Bouten et al., 2005, Choi et al., 2008, Crawford, 2005). Furthermore the mechanical mismatch between the viscoelastic polymer substrate and the brittle TCO anodic material may result in cracking and/or delamination during manufacture or operation (Crawford, 2005). The cracking of this brittle layer results in a decrease of the electrical functionality of these flexible devises and it is therefore it is critical that we conduct electro-mechanical tests to find the limits of these polymer/TCO systems.

1.2 Aims of the project

1) To investigate the effect of acrylic acid exposure on the electrical and optical properties of ITO coated PET substrates for thin films; as these systems can come into contact with numerous acidic environments during the manufacturing process and acrylic acid is commonly found in epoxies used to stack these systems during device manufacture. The optical reliability of these systems is vital during service; therefore any detrimental effects to these optical properties need to be fully understood.

2) To analyse the electro-mechanical behaviour of these thin films before and after exposure to an acrylic acid environment. During manufacturing processes, such as roll-to-roll processing, these devices will be exposed to a range of stresses including but not limited to; tensile and compressive bending whilst being exposed to acidic environments. It is therefore imperative that we investigate and compare the effects these scenarios may have on the system's ability to function effectively.

3) To investigate how the tribological properties of these thin film systems can be affected after exposure to acrylic acid. When these systems are stacked during the manufacturing process there is a possibility that they may slide past one another, furthermore the designed function of the device may require it to operate in a sliding motion. Therefore a detailed understanding of the tribology of these systems is required.

2. Literature review

2.1 Scope of this work

To fully understand how factors such as acrylic acid exposure affect the performance of commercial ITO/PET systems such as; the optical, electro-mechanical and tribological properties and the implications these affects cause on the fabrication and application of flexible display technologies, it is imperative that one fully understands the work that has been previously conducted within this area of research. This chapter aims to review relevant work conducted from within this field of study; from material selection through to device application, so that the effects of acrylic acid exposure on the ITO/PET systems ability to function effectively within flexible display technologies can be fully understood.

2.2 Potential substrates for use in flexible displays

For a substrate to be considered as an alternate for traditional glass substrates and to be used in new flat, flexible display technologies, it must match the current desired requirements. These requirements include;

- High optical transmission; the substrate needs to be optically clear in the visible spectrum.
- Low surface roughness as the electrical sensitivity of thin devices is sensitive to the substrates surface roughness.
- Good mechanical properties including a relatively high modulus enabling support for the device.
- Protection against the permeation of oxygen and chemicals.
- Desirable electrical properties, as the conductive substrate layer is commonly used as an anode.

Research into the development of flexible displays initially suggested that thin glass, metal foils and polymers can be considered as possible substrate developments. Thin glass films can allow a degree of flexibility and share the commonly desired properties of current glass substrates but are very brittle (Weber A, 2002). The brittle properties of the thin glass substrates limit their ability to be used in applications, thus not making them a viable substrate option. Research into metal foils has suggested that they are able to survive high process temperatures resulting in good barrier layers to both oxygen and moisture without the limiting brittle failure mechanisms of thin glass substrates, however they are very expensive, cannot handle multiple bends and are more suited for use in non-transmissive displays (Shin, 2005). The limiting factors with metal foil substrates however lie within the fact that they can only work in non-transmissive displays, cannot function with multiple blends and result in higher

manufacturing costs due to the increased cost of the material (Choi et al., 2008). Therefore polymers offer the best combination of both the desired properties including good optical, chemical and mechanical performances with a low material and manufacturing costs and the ability to be mass produced into the consumer market by a roll-to-roll process.

2.1.3 Potential polymer substrates for flexible displays

There are numerous polymers that could be considered as viable flexible substrates for flexible displays. The most commonly researched however are semi crystalline thermoplastics such as polyethylene terephthalate (PET), polyethylene naphthalate (PEN) and an amorphous thermoplastic, poly-carbonate (PC). The structure of these polymers is shown in Figure 2. 1.

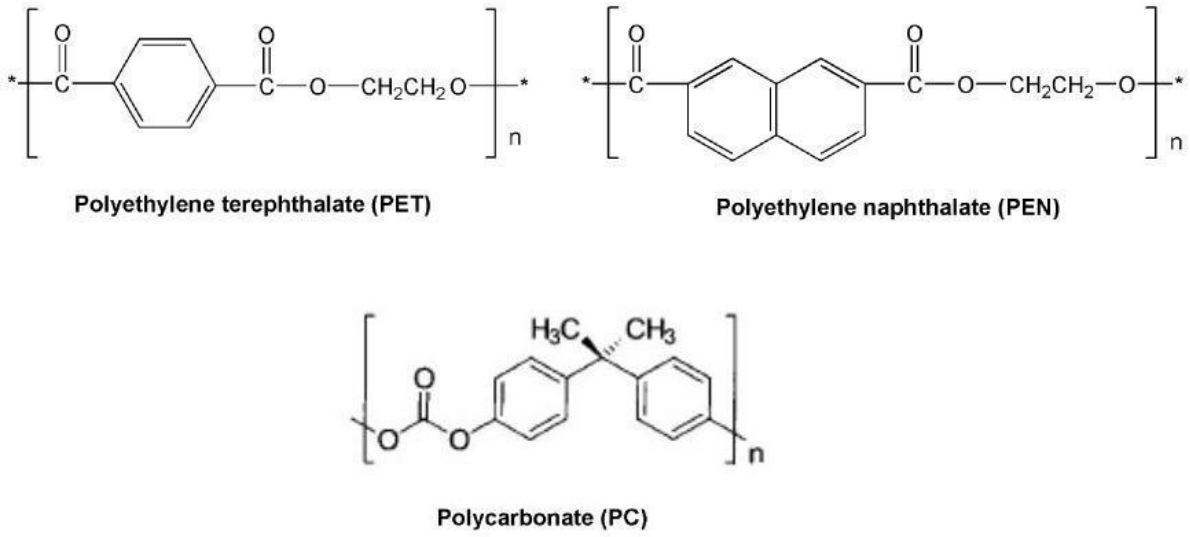

Figure 2. 1 Potential polymers that can be used as flexible display substrates (Choi et al., 2008)

The polyester polymers (PET and PEN) share the advantages of exhibiting high optical transmission, a desired coefficient of thermal expansion (CTE), provide a suitable barrier of chemical resistance and are relatively cheap to manufacture. However they also are subjected

to the disadvantages of having poor surface roughness and lower than desired glass transition temperatures (Tg) and upper operating temperatures, 150^{o}C and 200^{o}C for PET and PEN respectively. The knowledge of potential polymers glass transition temperature is vital in the material selection process, if the glass transition temperature of these polymers were to be above ~140^{o}C they would be subjected to a significant degree of degradation during melt-processing (Choi et al., 2008). Poly-carbonate on the other hand, offers improved surface roughness with excellent optical transmission properties, however when compared to both PET and PEN, has poor solvent resistance, poor mechanical properties with a similar upper operating temperature (150^{o}C) (Choi et al., 2008).

2.1.4 Alternate potential polymer substrates for flexible displays

As previously stated, the most commonly researched polymers for use in flexible display technologies are; PET, PEN and PC. However there are numerous polymer substrates that could potentially be used as the substrate material for these flexibly display technologies such as; polynorbonene (PNB), polyimide (PI), polyarylate (PAR), polyethersulphone (PES), polyether-etherketone (PEEK) an, polycyclic olefin (PCO) (Choi et al., 2008, MacDonald, 2004). Polyether-etherketone (PEEK), much like PET and PEN is a thermoplastic semi-crystalline polymer and polyethersulphone (PES) is an amorphous polymer which can be solvent cast or melt extruded. The following polymers, although amorphous, cannot be melt processed; polycyclic olefin (PCO), polyarylate (PAR), polynorbonene (PNB) and polyimide (PI). A detailed description of these polymers is not within the scope of this work.

2.1.5 Production of polyethylene terephthalate

Polyethylene terephthalate is a thermoplastic polymer that is widely used due to its ability to be recycled, satisfying the growing need for “greener” alternative to the commonly used

polymer. It was first made commercially available by a patent in 1941 from John Whinfield of the Calico Printers Association (Sierros, 2006). Early productions of PET were manufactured by reacting terepthalic acid with ethylene glycol. PET films can be produced via a number of methods but a drawing process is most commonly used. In this drawing process the temperature is taken above the polymers glass transition temperature (Tg) allowing melt extrusion through a slot die, quickly followed by quenching and as a result forms an amorphous precursor film. In-line drawing in both the transverse and machine direction takes place, often involving reheating above 80^{o}C, and is followed by in-line heat setting. During the in-line drawing in the transverse and machine direction, strain-induced crystallisation of up to 50% can be achieved (Sierros, 2006).

2.1.6 Chemical resistance of polyethylene terephthalate

During the manufacturing process polymer substrates will be exposed to a wide range of chemicals as well as moisture, therefore it is important that any polymer substrate to be used in thin flexible displays offers a strong resistance to moisture and solvents. Semi-crystalline polymers such as PET offer a strong to resistance to solvents such as acetones, methanol and acids, whereas amorphous polymers often have poor solvent resistance (Choi et al., 2008). PET can absorb 1400ppm O_2 at equilibrium however the exact values can fluctuate and are dependent on temperature and humidity.

2.1.7 Optical clarity

Optical clarity is one of the most important properties for display technologies. Crawford (2005) discussed the importance of the polymer substrates exhibiting an optical clarity of above 85% in the visible spectrum combined with a low haze value. PET offers total light

transmission of above 85% in the visible spectrum coupled with a haze value of less than 0.7% (MacDonald, 2004).

2.2 Transparent conducting oxides

Transparent conducting oxides (TCO) are currently used in a vast number of commercial flat-panel display applications such as; personal hand-held devices, televisions and computers to name just a few. One of the most commonly used of the TCO family is indium tin oxide. It is widely acknowledged as a transparent conducting electrode material due to its high optical transmittance of over 90% in the visible spectrum whilst being able to exhibit low electrical resistivity of 2×10^{-4} Ω/cm (Choi et al., 2008). These properties were obtained from ITO deposited onto glass substrates under high processing temperatures of 300 ^{o}C. However ITO thin films are very expensive due to the rarity of Indium and require high processing temperatures to achieve the desired optical and electrical properties on glass substrates. Moreover, they are extremely brittle, which causes problems in the application to thin flexible substrates.

For thin flexible displays to be commercially viable, they need to mirror the key properties of its glass counterparts, but deposition of TCO onto polymer substrates requires lower deposition temperatures (under 200^{o}C). It has been generally stated that by using lower temperatures during the deposition process will result in poor optical transmission and high electrical resistance (Kim et al., 2001). Techniques have now been developed to overcome these disadvantages of deposition at low temperatures. The pulsed laser deposition (PLD) deposition technique operates by using a high-powered pulsed laser beam focused on to a target material inside either a vacuum of background gas chamber. The latter is most commonly used with oxygen when depositing oxides to fully oxygenate the deposited film.

As the laser energy density reaches the required threshold a laser-induced plasma plume is produced resulting in the material being vaporised from the target and deposited onto the substrate as a thin film (Kim et al., 2001). By using this deposition technique Kim et al. (2001) stated that it was possible to obtain the key properties of high temperature deposition at low substrate temperatures of under 100oC. Kim et al. (2001) recorded electrical resistance as low as 4 x 10-4 Ωcm and an average optical transmission of 90% in the visible spectrum

The PLD technique was further developed by Chung et al. (2004) who depositing TCO's at room temperature followed by an annealing process using an XeCl excimer laser. The results of using excimer laser annealing were that the optical and electrical properties could be significantly improved when compared with other room-temperature deposition techniques. Other deposition techniques such as ion beam assisted deposition and reactive DC-Magnetron sputtering have also been reported to exhibit desirable properties (Young-Soon Kim and Shin, 2003). Although the PLD process can achieve highly desired properties for coated thin films such as a low surface roughness at low deposition temperatures, the limited area of the ablated plume eliminates the possibility of mass production.

2.2.1 The DC-magnetron sputtering process

Dc-magnetron sputtering is a commonly applied process as it enables large areas of thin films to be coated in a batch process. During this sputtering process gas ions are accelerated towards a target material from excited plasma, particles of the target material are then removed from the target material and condensed on to the desired substrate. This process takes part inside a vacuum chamber and a schematic diagram can be seen in Figure 2. 2.

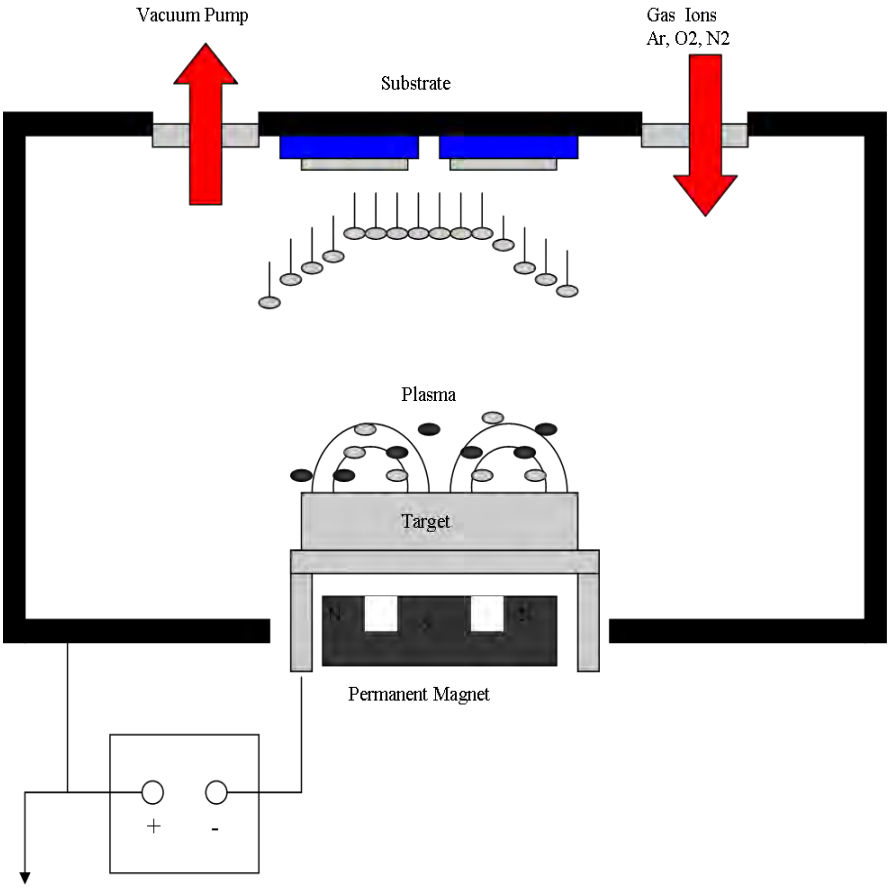

Figure 2. 2 A schematic diagram of the sputtering process

A reactive gas such as Argon is fed into the chamber to initiate the ignition of the plasma and due to radiation ionized Ar+ions become available. A high negative potential is applied to the target material and as a result the Ar-ions are accelerated towards the target and the material particles are removed, this can also produce secondary electrons causing additional ionization. Once the material particles are ionized, they are bombard and coat the substrate. A combination of the gas pressure and the electron distance can affect the probability of ionization and the introduction of the permanent magnet can increase the ionization rate by emitted secondary electrons even further. The magnet causes the electrons within its field to become trapped and circulate over the target surface for a longer period of time (Lan et al., 2009). This time increase results in a high possibility of ionization, forming plasma initiation at low pressures, which further results in higher deposition rates (Lan et al., 2009).

2.3 Roll-to-roll manufacturing

Currently the proposed method for the commercial production of display panels is via a lengthy batch process using vacuum deposition techniques such as dc-magnetron sputtering. However if a commercially viable roll-to-roll process could be developed, then this enables the manufacturing of thin flexible displays to produced at increased rate. The increase in the rate of production of these thin films results in a more viable processing method for consumer market expansion.

There are many advantages to the use of a roll-to-roll process;

- Total manufacturing overhead time will be significantly reduced as it will not be required to load and unload the display panels into the vacuum chamber or chemical processing stations.
- Contamination levels will be decreased with the reduction of contact during the loading and unloading phases.
- Due to the reduction in human contact in processing the substrates greater yields can be achieved.
- A greater degree of automation can be achieved.
- It will enable a one-step manufacturing process

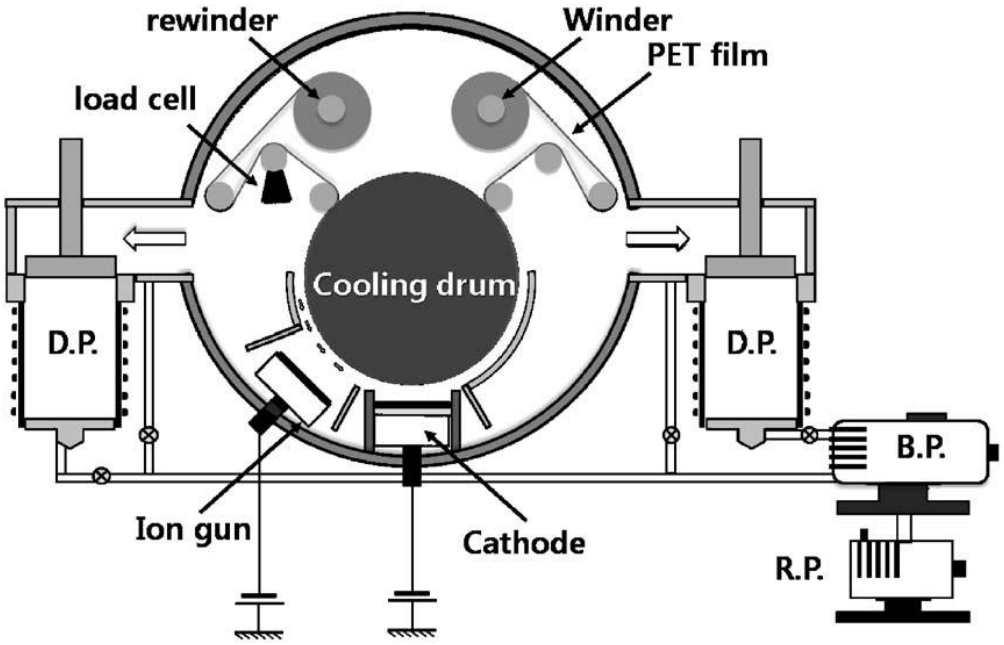

Figure 2. 3 Schematic diagram of a unique roll to roll sputtering system courtesy of (Choi et al., 2009).

Choi et al. (2009) developed a unique roll to roll sputtering system to coat polyethylene terephthalate substrates with indium tin oxide electrodes for the production of flexible organic solar cells. The roll to roll sputtering technique was able to deposit 200 mm wide PET substrates with a thickness of 188 μm with an Indium Tin oxide coating of 200 nm. A schematic diagram of the roll to roll sputtering process can be seen in Figure 2. 3. Choi et al. (2009) found that the optical and electrical properties of the indium tin oxide were dependant on the Argon/Oxygen flow ratio in this roll to roll process and even at low deposition temperatures films can be produced with a low sheet resistance (47.4 Ω/□) with an average optical transmittance of 83.46% in the wavelength region of 500 – 800 nm.

2.3 Indium tin oxide and flexible displays

It has been previously discussed that thin metallic foils can be used as the anodic material in flexible display technologies (Choi et al., 2008), however these materials can only obtain limited optical transmission properties whilst displaying an acceptable reduction in conductivity. Wide band gap (Eg > 3eV) materials such as ITO offer both high transparency and high electrical conductivity. ITO is formed via the doping of In_2O_3 with Sn which in turn replaces the In^{3+} atoms from the cubic structure of Indium Oxide (Fan and Goodenough, 1977). During this process Sn forms an interstitial bond with O_2 and exists as SnO or SnO2 with a valence of +2 or +4 respectively (Fan and Goodenough, 1977), and this valence directly influences the conductivity of the ITO layer where; a low valence results in a reduction in conductivity as a result of a decrease in carrier concentration and a high valence results in an increase of conductivity due to Sn^{+4} acting as an n-type donor releasing electrons (Paine et al., 2005). The high optical transmittance values of ITO film properties are due to the material being a wide band gap semi-conductor. However these values can be influenced by a number of defects such as surface roughness and a high deficiency of oxygen atoms can reduce the size of the band gap and therefore results in a reduction of the films transparency and carrier mobility (Kim, 2007)

2.3.1 Mechanical properties of ITO coated polymer substrates

The advantages of using ITO as the transparent conducting oxide for thin flexible display technologies has been previously discussed, however the mechanical properties of the material influence the development and production of these technologies. It is known due to the rarity of indium, that manufacturing costs are high, and also the brittle nature of ITO induces problematic situations when discussing the manufacture of thin flexible displays. Therefore investigation into the mechanical failure of the thin film materials is vital in the selection process for coated polymer substrates to be considered for use in thin flexible display technologies.

Previous research into the electro-mechanical properties of ITO coated polymer substrates such as investigating the strain – dependant electrical resistances of ITO have shown that at a certain strain percentage, electrical resistance of the ITO coated polymer substrate increases rapidly (Cairns et al., 2000). This strain threshold is known as the critical onset strain (COS) and occurs due to crack formation and propagation in the ITO layer and is defined as the strain at which the increment of electrical resistance measured *in situ* is equal to 10% (Bouten et al., 2005, Leterrier, 2003). Three PET substrate samples were used in an initial investigation with varying sheet resistances of 80, 200 and 500 Ω/square which correlates to a coating thickness of 105, 42 and 16.8 nm respectively (Cairns et al., 2000). Low sheet resistance such as 80 Ω/square correlates to a thicker ITO coating (105 nm) and the results display not only a rapid electrical increase at a certain strain percentage but also that the thickest ITO coating investigated (105 nm) failed at the lowest stain percentage, inferring that the critical onset strain is dependent on the ITO film thickness. This work was continued further by Cairns D.R. (2001) where thin ITO films of varying sheet resistances from 61 –

400 Ω/square were deposited on to a 125 μm thick PET substrate via DC magnetron sputtering. Uniaxial tensile tests using a miniature tensile testing machine (Rheometric Scientific Minimat 2000) were performed whilst electrical resistance was measured *in*-situ, and an optical microscope enabled optical analysis of crack propagation. The results showed crack initiation occurs perpendicular to the load direction at a COS of 2.75%. As the strain in the sample is increased above this critical onset strain, the number of cracks rapidly increases, resulting in a decrease in fragment length and a rapid increase in electrical resistance. The tensile properties have been further researched using a tensile and 2–point bend testing method to discover the critical failure strain of ITO coated polymer substrates (Bouten, 2002). Two polymer substrates of 100mm and 22mm in sample length were used with a constant ITO coating thickness of 100nm and the electrical resistance was monitored *in-situ.* Results showed that the critical onset strain (COS) determined as a 10% increase in electrical resistance was observed at 2.3% for the 100 mm sample and 5% for the shorter 22 mm sample. The differences in critical onset strains were attributed to clamping issues. The 2–point bend test displayed failure strains of 1.29% and 1.21% for the 100 mm and 22 mm samples respectively, significantly lower than the failure strains shown in the tensile tests.

The film thickness dependence of the electro-mechanical and optical properties of ITO thin films have been systematically investigated using film thicknesses of 72 nm to 447 nm on polyethylene terephthalate substrates (Hao et al., 2008). Through XRD and SEM analysis it can be seen that the crystal grain size and surface roughness increases with an increase in film thickness. However the optical transmission and sheet resistivity decreases with an increase in ITO film thickness, due to the crystal grain structure becoming too large. It should also be noted that thick ITO films exhibit a lower COS than thinner ITO films, which is consistent

with previous studies where the COS has been seen to be inversely proportional to the square root of the film thickness (Cairns D.R., 2001, Wang et al., 1998, Hao et al., 2008) This confirms that the mechanical properties of ITO coated polymers substrates for use in thin flexible displays are dependent on the ITO film thickness.

When a thin flexible display component is flexed during service, further mechanical complications arise. As the component is flexed, one surface will be under compressive strain whilst the other in tensile strain. However at the centre of the film lies a neutral axis where stain will equate to zero (Chen et al., 2001a). At any other layer away from the centre of the film however the strain can be given by;

$$\boldsymbol{\varepsilon = \frac{\gamma}{R}} \tag{2. 1}$$

where γ is the distance away from the neutral axis and R is the radius of curvature of the neutral axis.

Therefore it can be seen that one can maximise the flexibility of the device by ensuring that the brittle ITO layer is close to the neutral axis (Z. Suoa, 1999). However if the ITO layer is unable to be placed close to this neutral axis, then the component will be limited by the brittleness of this layer and a further understanding of the fracture properties and failure mechanisms is required. Chen et al. (2001a) used ITO coated PET substrates under simply supported ends and clamped situations and induced both tensile and compressive stresses via a series of bending experiments. Chen et al. (2001a) results showed that if the sample was placed under tension a steady state channelling crack is formed, however if the sample was

placed under compressive loads, the ITO coating delaminates and buckles before cracking propagates. It was said that under low power microscope analysis the failure mechanism for compressive loads was superficially seen to be similar to tensile channelling cracks, however under further high magnification (Scanning Electron Microscopy) surface analysis the failure mechanism is shown to be a tunnelling – delamination – buckling – crack. The mean critical onset strains for tensile and compression were found to be 1.1% and 1.7% respectively, however whether the tensile or compressive strain is more critical is dependent on the cracking resistance energy to delamination toughness ratio, G_c/G_d (Chen et al., 2001a, Chen et al., 2002). When the sample is under a uniform applied strain and the length of the channelling crack is greater than the film thickness, then steady – state cracking may be observed (Chen et al., 2001a). During steady – state cracking the crack length does not affect the level of applied strain as the energy release rate is constant (Chen et al., 2002, Chen et al., 2001a). Therefore the ITO layer will fail if its release energy is either greater or equal to this crack resistance energy (G_c) (Chen et al., 2001a, Bouten et al., 2005) where G_c is given by (Hutchinson, 1996, Beuth Jr, 1992, Chen et al., 2002);

$$\boldsymbol{G_c = \frac{1}{2}\bar{E}_f \varepsilon^2 \pi h_f g(\partial, \beta)} \quad (2.2)$$

where $g(\partial, \beta)$ is a function of the Dundur's parameter shown in equation 3 for plane strain conditions;

$$\boldsymbol{\alpha = \frac{\bar{E}_f - \bar{E}_s}{\bar{E}_f + \bar{E}_s}} \qquad \boldsymbol{\beta = \frac{\bar{E}_f\left(\frac{1-2\nu_s}{1-\nu_s}\right) - \bar{E}_s\left(\frac{1-2\nu_f}{1-\nu_f}\right)}{2(\bar{E}_f - \bar{E}_s)}} \quad (2.3)$$

When thin films are placed under compressive loads the brittle ITO layer may also delaminate via a buckling mechanism. Within this buckling mechanism the elastic energy stored within thin film is released resulting in a new free surface by peeling the coating from the substrate surface (Bouten et al., 2005). Chen et al. (2002) placed samples under compressive loads and investigated their failure mechanism features using SEM and AFM, the images revealed that the failure mechanism was that of a buckling delamination closely followed by film cracking. In compression the energy release rate is based upon the delamination area and is given as (Chen et al., 2000, Chen et al., 2002, Chen et al., 2001a);

$$\boldsymbol{G_t = G_d + \left(\frac{h_f}{2b}\right) G_c} \tag{2. 4}$$

where G_d is the delamination energy, G_c is the crack resistance energy and $2b$ is the delamination width. As previously mentioned the cracking resistance energy to delamination toughness ratio, G_c/G_d dictates whether the thin film will fail fist in either tension or compression. If $G_c < G_d$ then tensile failure may occur at a lower strain than under compression (Chen et al., 2002, Chen et al., 2001a).

Stress – corrosion cracking failure mechanisms under applied bending strains were investigated by Sierros et al. (2009b) via wrapping samples around mandrels that ranged in differing diameters. These samples were then submerged in differing concentrations of acrylic acid solutions. The results showed a reduction in the electrical properties of the thin film samples due to corrosion induced cracking, furthermore as the acidic concentration increased, so did the degree of corrosion. As a result of this, when a bending strain was

applied it could be seen that the thin film samples failed significantly sooner than the samples that were just subjected to corrosion with no applied stress. With this in mind it was observed that the combination of both an applied stress and a corrosive environment, cracking of the ITO layer can be initiated at stresses of less than a quarter of those needed without corrosion.

Lan et al. (2010) further investigated the failure mechanisms during bending conditions and aimed to improve the optical and electrical properties of ITO coated PET substrates for use in thin flexible displays via the use of a thermionic emission (TE) enhanced DC magnetron sputtering system. X-ray diffraction patterns showed that the samples without a thermionic emission layer displayed an amorphous feature whereas the samples with a TE layer demonstrated a clear crystalline structure (Lan et al., 2010). The presence of this crystalline region is as a result of substrate temperature elevation in combination with an intensified plasma density (Lan et al., 2009). Bending tests showed that via the inclusion of TE layers, mechanical and adhesive properties can be significantly increased; the critical radius of curvature improved from 17.00 mm to 13.9 mm, samples could perform above 1200 rhythmic cycles compared to just 50 and the optical transmission was seen to have improved from 70% to 83%. The increase in these mechanical properties is due to the increase in crystallinity and film adhesion during the sputtering process (Lan et al., 2010).

2. 4 Tribological properties

Flexible display devices are diverse in their function and application selection, so it is therefore expected that flexible display devices may need to effectively function in a range of harsh environments such as; in solar panel technologies or the automotive industry to name but a few. Cairns D.R. (2001) investigated the adhesive wear of ITO coated PET substrates. A polymer stylus was repeatedly drawn over the sample for 60,000 siding cycles. This resulted in pit formation in the ITO layer with polymer extrusion through the ITO pits and ITO flakes from the top surface to the bottom surface. With an increase in the number of sliding cycles crack formation was observed.

When ITO anodes become exposed to voltage differences in the presence of moisture and contamination, their resistance to corrosion is decreased (Sierros et al., 2009a). Moreover the components of the flexible display device can come into contact with acidic solutions from either harsh environment conditions or epoxy resins, these acidic solutions can corrode the brittle ITO layer and any applied or residual stresses can result is stress corrosion cracking, resulting in crack formation, propagation and/or delamination (Sierros et al., 2009a).

Sierros et al. (2009a) further investigated the tribological properties of ITO coated PET substrates through a custom built reciprocating wear testing rig under both dry and wet sliding conditions, where a flat ITO surface came into contact with another flat ITO counter surface. During the experiment the top sample slides in a reciprocating motion over the bottom surface and for wet sliding conditions the sample was placed into a container filled with a 0.1 M acrylic acid solution with a constant applied load of 3.5 Newton. At 100 sliding cycles a 40% resistance increase was observed and at 10,000 cycles a large rapid increase in electrical

resistance was seen which indicates a significant loss of surface functionality. Microscopy evaluation revealed plastic deformation of the underlining polymer substrate and crack formation with a 45 degree orientation with respect to the sliding direction, which infers that the wear mechanisms of the ITO surface include cohesive failure within the film and adhesive wear between the ITO film coating and the PET substrate (Sierros et al., 2009b, Sierros et al., 2009a).

Solar panels applications are highly at risk to the exposure to harsh environmental conditions and their efficiency and long term reliability are dependent on the surface integrity of the film which can be damaged due to their exposure to harsh environmental condition (Sierros et al., 2011). Sierros et al. (2011) investigated the efficiency and long term durability of multilayered Ag/Ag – alloy based ITO thin films via the use of a reciprocating wear test. A polytetrafluoroethylene ball, commonly known as PTFE was reciprocated over a thin film under wet sliding conditions with the use of a NaCl solution (1 M concentration) under moderate loading conditions (3 N) and by increasing the number of cycles (3 cycles/minute). The reciprocating motion of the PTFE ball; chosen due to its low friction coefficient, was of 25.4 mm in length and due to the load a mean Hertzian contact pressure of 0.56 MPa was induced, which is a typical contact pressure under moderate handling and service conditions for solar panel components (Sierros et al., 2011). The investigation discovered that; critical onset crack formation initiated between 200 and 268 cycles, over 3240 cycles resulted in a decrease in mass of the PTFE ball due to wear transfer and impregnation onto the thin film sample, an increase in reciprocating cycles results in the corrosion resistance of the sample decreases and with regards to weight measurements three wear regimes are inferred up to 540, up to 1080 and above 1080 reciprocating cycles respectively.

2.5 Hertzian contact mechanics

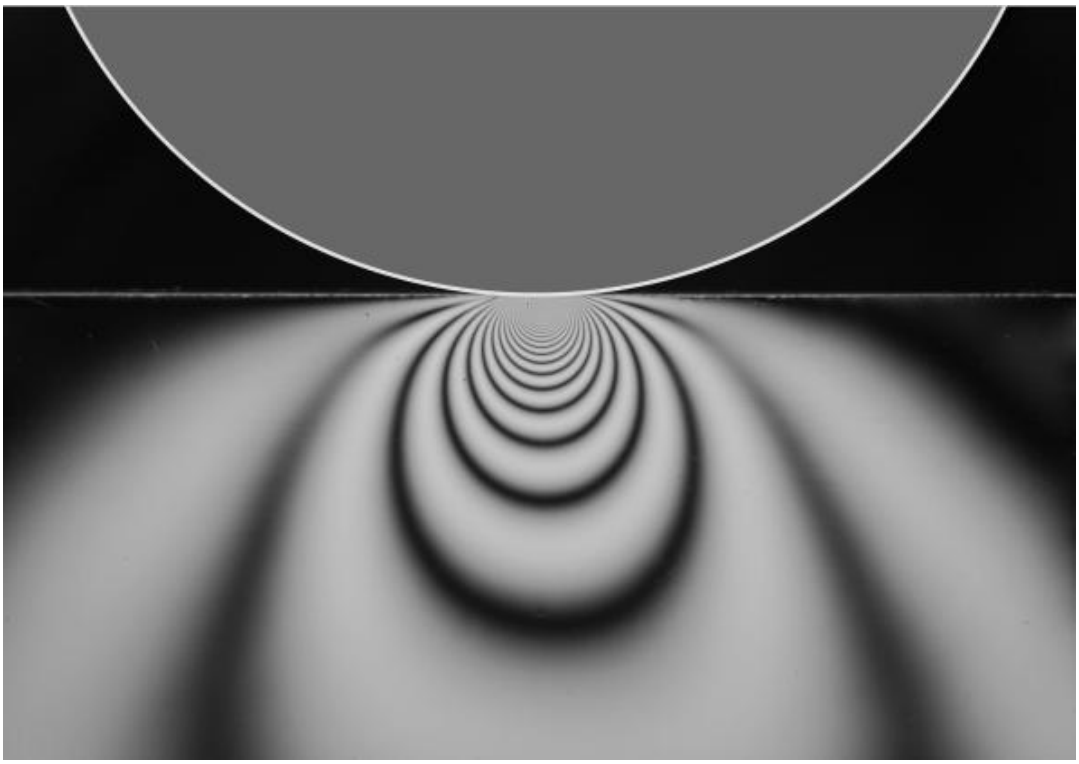

Image courtesy of (Popov, 2010)

Contact mechanics is the study of the stresses, deflections and deformations of two elastic solids that touch each other and require particular attention in hardness, impact and wear testing (Fischer-Cripps, 1999). The mathematical formula is built upon the mechanical properties of the materials used and mechanics where elastic, viscoelastic and plastic bodies are in either dynamic or static contact (Popov, 2010). A common area of interest is in the contact between a flat specimen surface and a rigid indenter. The indenter can consist of a number of shapes including spherical or cylindrical to name but a few and is commonly referred to as “Hertzian contact” (Fischer-Cripps, 1999).

This project will be investigating a rigid sphere indenter on a flat surface scenario where Hertz (1896) found;

Radius of the circle of contact

$$\boldsymbol{a^3 = \frac{4}{3}\frac{kPR}{E}} \tag{2. 5}$$

Elastic mismatch factor

$$k = \frac{9}{16}\left[(1 - v^2) + \frac{E}{E'}(1 - v'^2)\right] \tag{2. 6}$$

Maximum tensile stress of the specimen

$$\sigma \max = (1 - 2v)\frac{p}{2\pi a^2} \tag{2. 7}$$

Maximum tensile stress outside the indenter given in terms of indenter radius R

$$\sigma \max = \left(\frac{(1-2v)P}{2\pi}\right)\left(\frac{3E}{4K}\right)^{2/3} P^{1/3} R^{-2/3} \tag{2. 8}$$

Mean contact pressure

$$Pm = \frac{P}{\pi a^2} \tag{2. 9}$$

Indenter stress in terms of mean contact pressure, given by substituting equation 2.9 into equation 2.5

$$Pm = \left(\frac{3E}{4\pi K}\right)\frac{a}{R} \tag{2. 10}$$

With regards to equation 2.5, *a*, is related to the indenter load *p*, radius *R* and the elastic properties of the indenter material. Equation 2.6 expresses the elastic mismatch factor where; *E* is the Young's modulus of the specimen, E' is the Young's modulus of the indenter and *v*, *v'* represent the Poisson's ratio of both the specimen and indenter respectively. Poisson's ratio, also known as the Poisson effect occurs when a sample is stretched and is the ratio of the transverse strain perpendicular to the applied load to the axial strain in the direction of the applied load (Lakes, 1987). During the contact between the indenter and the specimen the maximal tensile stress of the specimen occurs at the edge of the circle of contact and is given in equation 2.7. Due to the stresses that occur and act in a radial direction on the surface of the specimen, Hertzian Zone Cracks can occur if these stresses decrease to the inverse square of the distance away from the centre of contact (Fischer-Cripps, 1999). The maximum tensile stress outside of the indenter can be expressed in terms of the indenter radius by combining Equations 1 and 3 and is shown in equation 2.8. Hertz, 1896 found a normalising parameter, the mean contact pressure, *Pm,* given by the indenter load/contact area. The mean contact pressure is expressed in equation 2.9. With this information in hand it can be seen that the contact area is proportional to $P^{2/3}$ and therefore *Pm* is proportional to $P^{1/3}$. We can then substitute equation 2.9 into equation 2.5 and the mean contact pressure can be referred to as the indenter stress and the quantity (*a/R*) as the indenter strain as shown in equation 2.10. The relationship shown between *Pm* and *a/R* in infers to an existence of a similar stress – strain responses observed in traditional tensile and compression experiments (Fischer-Cripps, 1999). As the substrate ids viscoelastic, it is assumed that the critical depth is not reached and therefore plastic deformation does not take place.

3. Materials and experimental methods

3.1 Sample preparation

3.1.1 Polymer substrates

Commercial polyethylene terephthalate (PET) polymer substrates that had been coated with Indium Tin Oxide (ITO) via sputtering techniques were placed under examination. The samples were in the form of A4 sheets of three varying sheet resistances; 50 Ω/□, 100 Ω/□ and 300 Ω/□. The samples were provided by Dr. Darran Cairns of West Virginia University USA and were manufactured by Solutia Films Incorporated (USA) where they used a commercial magnetron sputtering machine, coating the polymer substrates in batches.

The polymer sheets were separated from one another by paper sheets to avoid any surface damage to the surface layer. Examination gloves were be worn at all times when carrying out experiments or in general handling of the films to avoid damage and contamination. Samples were cut out of the A4 sheets using a sharp razor blade and a steel ruler.

For optical transmission and sheet resistance measurements 29mm/29mm square samples were made. The Moore hydraulic press was used with a cutting mould to produce the traditional dumbbell samples needed for tensile testing, monotonic bending and our designed fretting experiment. A section of the film was cut out using a razor blade and steel ruler and is then placed on top of the cutting mould. Thin card is then placed over the top of the sample so the process does not affect the polymer substrate and ITO coating properties. The procedure was carried out until two tons of pressure was reached.

Table 3. 1displays the number of samples tested at each varying acidic concentration for the experiments used in this investigation.

Table 3. 1 Sample numbers examined during this investigation

Acidic Concentration	Optical Transmission	Surface Resistance	Tensile Testing	Monotonic Bending	Fretting
No Acid	15	15	15	30	9
0.1 Molar	15	15	15	30	9
0.2 Molar	15	15	15	30	9
0.3 Molar	15	15	15	30	9
0.4 Molar	15	15	15	30	9
0.5 Molar	15	15	15	30	9
Total	**90**	**90**	**90**	**180**	**54**

3.1.2 Acidic corrosion

Acrylic acid ($C_3H_4O_2$) was used to corrode the ITO layer of the films. It has a molecular mass of 72.06 g mol^{-1} and a relative density of 1.05 g/ml at 25^{o}C. The acid was supplied by Sigma Aldrich. A stock solution was produced with a concentration of 1M. From this stock solution, varying concentrations of 0.1 M to 1 M can be easily produced. The samples were placed in a Petri dish submerged in 25ml of acrylic acid solutions from 0.1 M to 0.5 M and left in a well ventilated room and labelled accordingly.

3.2 Experimental methods

3.2.1 Sheet resistance measurement

The ITO-coated films were examined using a four point probe system. The system was composed of four tungsten probes aligned linearly with 1 mm probe spacing, an ohm-meter, a DC current source and a volt meter. The sample is placed on the base of the machine and the probe head is slowly driven down so the probes just come into contact with samples surface. With the probes aligned linearly, a current is applied to the outer probes and the two inner probes measure the voltage potential of the sample (Gutierrez, 2002). From this, the sheet resistance, R_s (Ω/□) is calculated using equation 3.1 (Runyan and Shaffner, 1997).

$$R_s = R \times \frac{\pi}{\ln 2} = R \times 4.532 \qquad (3.1)$$

A schematic diagram of the four point probe can be seen in Figure 3. 1. The resistance can vary slightly over the sample surface, so a minimum of ten measurements were taken on various areas of the samples at room temperature and an average was taken.

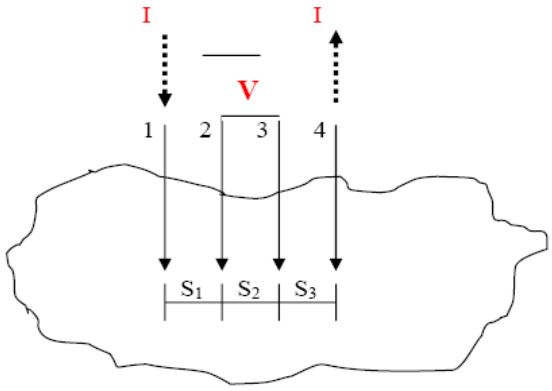

Figure 3. 1 The 4 - point probe alignment courtesy of (Gutierrez, 2002).

3.2.2 Optical transmission measurement

A Jenway 6315 spectrophotometer was used to measure the optical transmission of the samples. The spectrophotometer has a wavelength scan range of 198 nm to 1000 nm using a monochromatic light beam with a bandwidth of 8nm and exhibits a wavelength accuracy of ±2 nm. The monochromatic light beam is generated by a lamp and is focused onto the grating and is reflected into the sample chamber where it penetrates the sample and reaches the detector where the optical transmission is calculated at the given wavelength. A schematic diagram of this process can be seen in Figure 3. 2. Before measurements can be taken the machine must complete a baseline calibration.

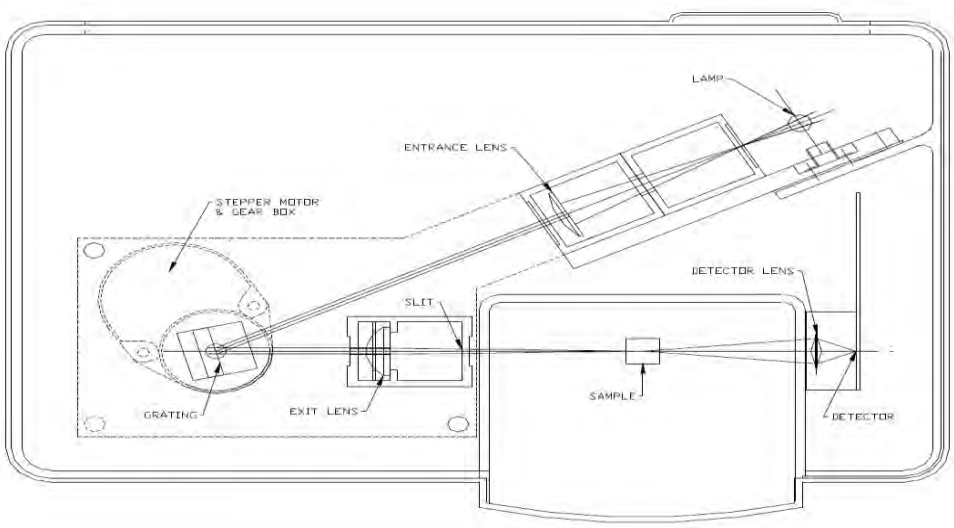

Figure 3. 2 Schematic diagram of the Jenway spectrophotometer process adapted from www.jenway.com

The samples were scanned between 250 nm and 1000 nm. The software measures the absorbance of the sample and the data can be manually converted to transmittance in a spread sheet program using equation 3.2 where A is the absorbance and T is the transmittance;

$$A = -\log T \tag{3. 2}$$

3.2.3 Tensile testing

Uniaxial tensile testing of the dumbbell samples were replicated using a modified Instron 5520 tensile testing machine shown in Figure 3. 3 (Potoczny, 2011). Two copper wires were connected to both the upper and lower grips of the Instron and are connected to resistance meter in order to measure the electro–mechanical properties *in–situ*. For these measurements to be taken a closed electrical circuit must be made using polytetrafluoroethylene (PTFE) screws to the base of the machine. The samples used in this method of testing are traditional dumbbell samples made using the Moore hydraulic press. The samples dimensions consisted of; a thickness of 0.197 mm, a width of 4 mm and a length of 18 mm. When mounting the samples within the grips care must be taken to ensure the film is completely vertical in the form of a 90^{o} angle with respect to the base. The applied stress - strain data points are collected by one computer using Merlin Software and the change in electrical resistance data points are collected via a separate computer running National Instruments Lab View software. The samples were subjected to strains at room temperature at a constant speed of 0.08mm/min to around 8% strain. The Failure of the ITO/PET system was characterised by a 10% increase in the increment of electrical resistance ($\Delta R/R_o$). This 10% increase relates to the critical onset strain where crack initiation occurs and begins to propagate.

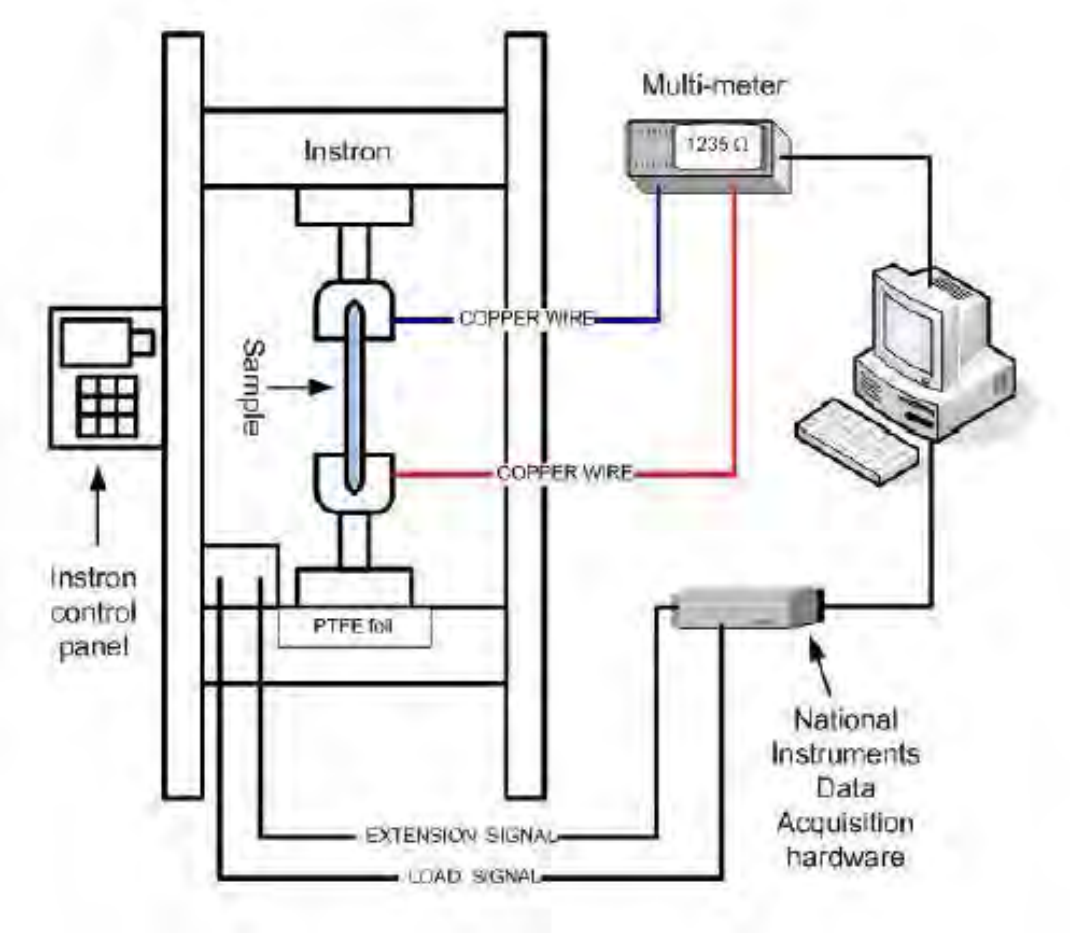

Figure 3. 3 Schematic diagram of the Instron Tensile Testing Experiment adapted from (Potoczny, 2011)

3.2.4 Monotonic bending

A free supported ends device was designed in this project by Grzegorz Potoczny and was used to investigate the flexibility of ITO/polymer systems. The designed grips were prepared and attached to the Instron tensile testing machine. The designed grips consisted of small smooth "crocodile" clips that were attached to a PTFE rod. These crocodile clips secure the sample during the experiment and are attached specifically so that they can freely rotate around their axis. Copper wires similar to the wires used in the tensile testing experiment were used to measure the change in electrical resistance *in situ*. This is achieved via the copper wires being attached to a resistance meter and any electrical resistance changes are again monitored by the Lab View software. The experimental set up can be seen in Figure 3. 5 (Potoczny, 2011).

The dumbbell samples with a dimension of 4 mm x 25 mm are then secured via the crocodile clips. A ruler is placed next to the sample to represent a scale when analysing the results and a camera is placed in front of the device to record the deformation profile of the samples. During the experiment the top rod is driven down at a speed of 2 mm/min causing the sample to bend. This device provides simple support for the sample's ends to represent true bending conditions, rather than the traditional clamping methods which results in the ends of the sample being deformed, with strain being induced and therefore not representing true bending.

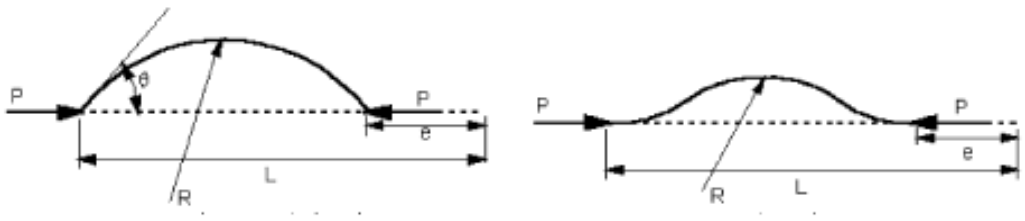

Simple supported end Clamped ends

Figure 3. 4 buckling testing scheme courtesy of (Chen et al., 2002)

The experimental set up can be seen in Figure 3. 5. Figure 3. 4 displays the difference between the simple supported end technique and the traditional clamping technique. The camera records images with a three second delay and we are able to measure the radius of bending curvature using equation 3.3; where *K(k)* and *E(k)* are the complete elliptic integrals of the first and second, $k = \sin(\theta/2)$, L is the original length, R is the radius of curvature and $\lambda = e/L$ the contraction ratio (Chen et al., 2002, Chen et al., 2001b). The critical onset radius (COR) is given as a 10% increase in electrical resistance.

Large deformation buckling theory of beams.

$$\lambda = 2\left[1 - \frac{E(k)}{K(k)}\right], \qquad \frac{l}{r} = 4K(k)k \tag{3. 3}$$

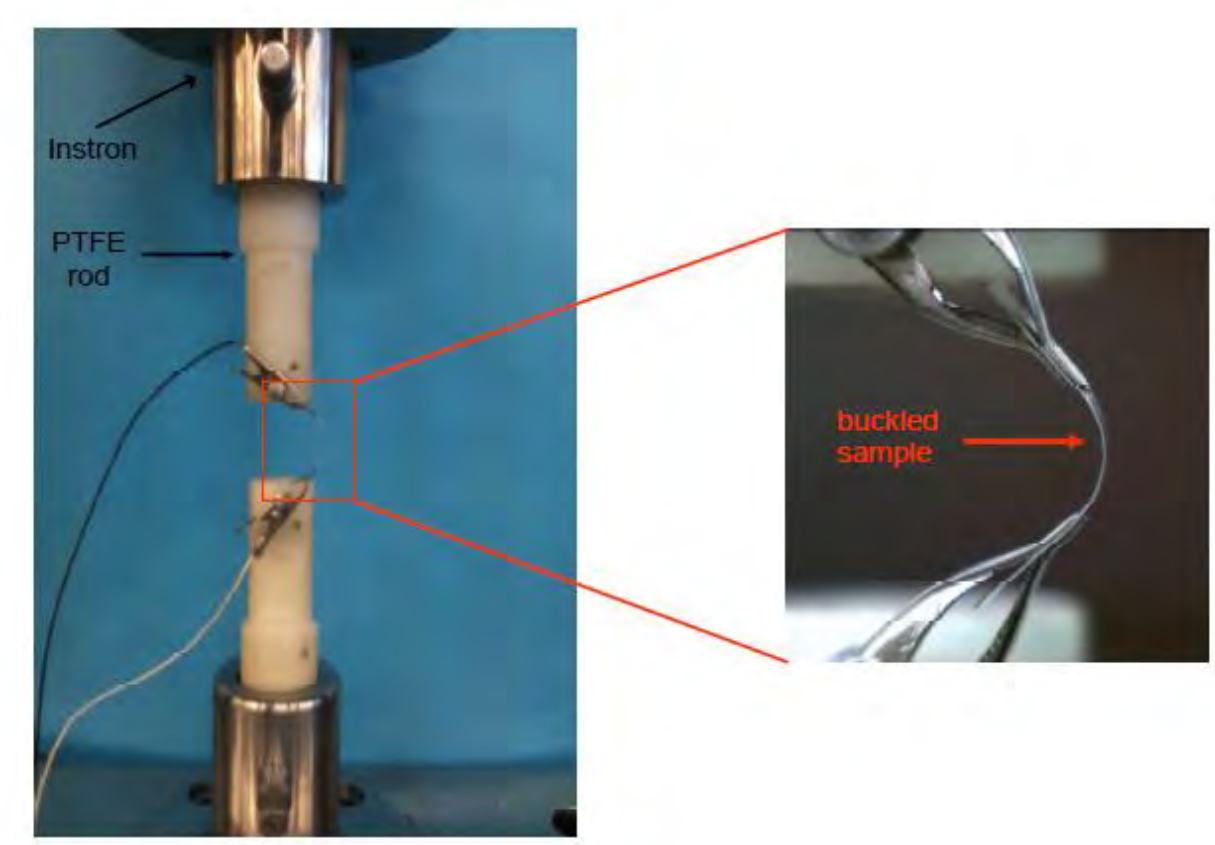

Figure 3. 5 Custom bending equipment with a buckled ITO/PET sample adapted from (Potoczny, 2011)

3.2.5 Tribological techniques

The tribological properties of thin film samples were investigated in this project using a reciprocating wear test. A High Frequency Reciprocating Rig (HFRR) was used to test the tribological properties and the change in electrical resistance was measured *in situ* using a resistance meter. The HFRR is a commonly used technique in mechanical engineering to test diesel and bio fuel lubricity; however for this a number of customisations were applied to allow for wear testing of the thin film samples to take place. Firstly, using computer aided design software (CAD) a customised specimen holder was produced with the help of Andrew Hoover from West Virginia University. The specimen holder was manufactured out of a thermosetting resin, Phenol formaldehyde, commonly known as Tufnell as future experiments will require testing in wet sliding conditions; including acidic solutions and Tufnell's material properties offer a high resistance to chemicals such as the acids we may be using. The dimensions of the specimen holder match the requirements needed by the HFRR chamber to ensure compatible testing conditions and can be seen in Figure 3. 6.

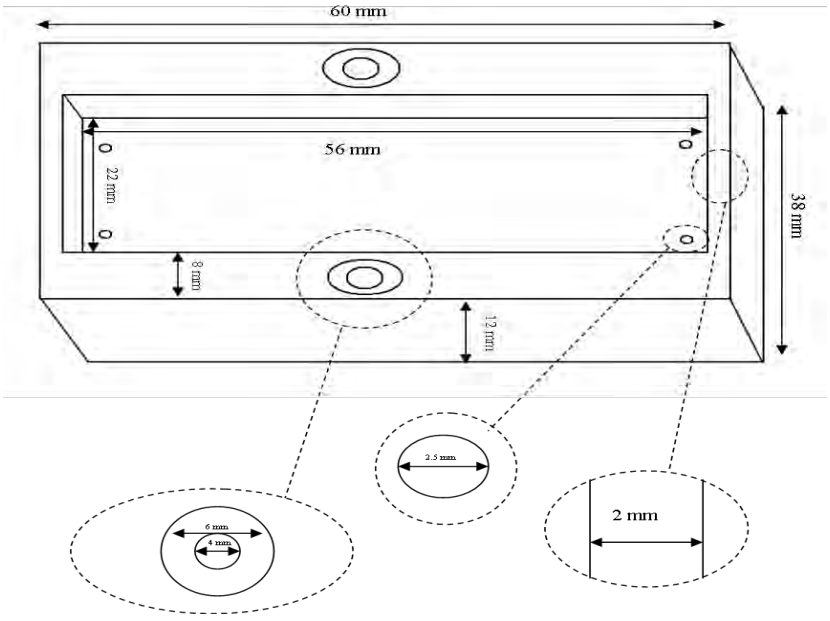

Figure 3. 6 A schematic diagram of the specimen holder and its dimensions

In traditional HFRR testing a steel ball bearing is used, however in this project a Polytetrafluoroethylene (Teflon) ball with a diameter of 6 mm was used. This allows us to easily detect any wear transfer via the detection of fluorine using energy-dispersive X-ray spectroscopy (EDS) and the softer surface of the polymer ball will not cause premature failure. The sample is fixed into the specimen holder via conducting metal clamps which can be seen in Figure 3. 7.

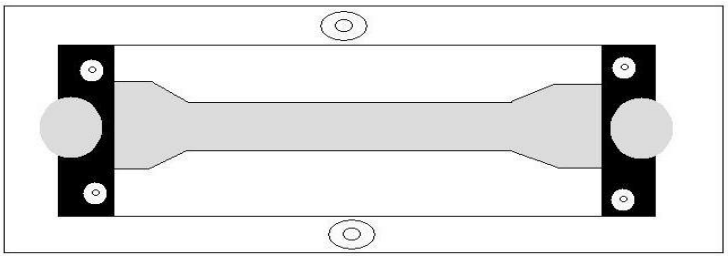

Figure 3. 7 Schematic diagram of the ITO/PET sample clamped into the specimen holder

Electrodes attach to the specimen holders metallic clamps which are in turn connected to a resistance meter and Lab View software, the holder is then placed into the HFRR testing chamber and secured. The PTFE ball is secured into a holder and then placed into the HFRR chamber. The testing parameters can then be set using computer software compatible with the HFRR. The following parameters were used;

- A load of 100g.
- A stroke length of 2 mm.
- A testing frequency of 10 Hz.
- Dry sliding conditions.
- Testing at room temperature.
- Time of the experiment was set to 30 minutes.
- Hertzian contact pressure of 0.32 MPa
- Assuming totally elastic deformation

Figure 3. 8 displays the schematic setup of the experimental process.

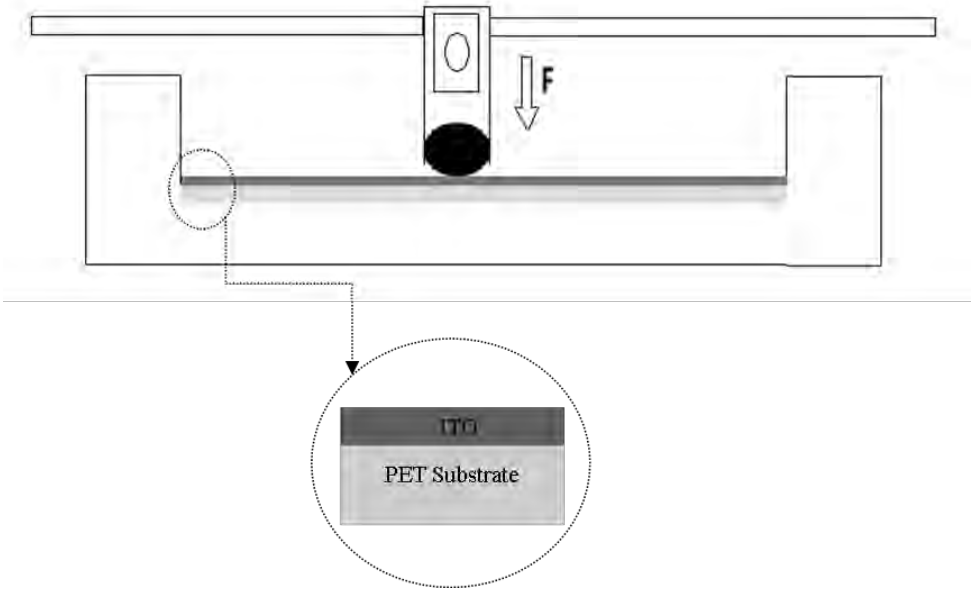

Figure 3. 8 A schematic diagram of the fretting process.

Surface analysis of both the thin film sample and the polymer ball can be examined using an optical microscope that is connected to the HFRR software. This allows for immediate analysis of the wear scars of both samples.

3.3 Surface analysis

3.3.1 Scanning Electron Microscopy (SEM)

The SEM was used in this project to investigate the surface morphology of the samples. SEM is a widely known and reputable technique that is commonly used in modern laboratories as it is able to produce a high lateral resolution with a combined good depth of focus. A conventional Joel 6060 microscope with a tungsten gun was used for surface analysis. Microanalysis is also available through energy dispersive x-ray spectroscopy (EDS), enabling the chemical characterisation of the ITO layer. Analysis was conducted with a working distance that was set to equal 10mm and the voltage can be changed between 0.5 – 30KV, however a standard voltage of 15KV was adopted. Prior to SEM analysis the samples were placed onto an SEM 'stub' and adhered with an adhesive disk. The samples are then gold sputter coated prior to investigation. Silver dag lines are also placed down the side of the sample to ensure a continuous electrical path from the sample to the 'stub'.

4. Results and discussion

4.1 Opto-electrical properties

4.1.1 Optical transmission

Samples were placed under optical examination using a Jenway Spectrophotometer that has previously been discussed in section 3.2.2. From each A4 sample sheet (OC50, OC100 and OC300) 30 smaller 29/29 mm square samples produced using a razor blade and a steel ruler. Of these samples, 25 were placed in an acrylic acid solution of 25ml varying from 0.1 to 0.5M for two hours and five reference samples were not exposed to any acidic environments.

Figure 4. 1 displays the transparency spectra of the samples that were not exposed to any acidic environments in the wavelength range of 318 to 1000 nm. It can be seen that the thickness of the brittle ITO layer has a direct effect on the optical transmission of the ITO/PET system in the visible wavelength spectrum 400 to 800 nm with the thinnest of the ITO layers (OC300) exhibiting the highest transparency spectra. The effect of acrylic acid was then investigated on the OC50, OC100 and OC300 samples and the effects of varying acidic concentrations on these samples can be seen in Figure 4. 2, Figure 4. 3 and Figure 4. 4. The apparent dip in optical transmission that can be observed between 318 to 418 nm is insignificant, it is only present as a result of the configuration settings of the Jenway Spectrophotometer, and therefore should be ignored.

It can be seen that the OC50 sample has been greatly affected by the influence of an acrylic acid environment, more so than the OC100 and OC300 samples. Samples exposed to 0.1 to

0.4 M for two hours, although exhibiting a significant increase in the level of optical transmission to the reference sample, did not show any significant changes in optical transmission between the varying levels of acidic concentration. However, samples exposed to an acrylic acid environment of 0.5 M for two hours, showed a significant increase not only from the reference sample, but also a greater degree of optical transmission than that of samples exposed to 0.1 to 0.4 M of acrylic acid. The OC100 and OC300 samples shared similar transparency spectra traits, such as minor increases in optical transmission from the reference samples to acidic exposure up to a 0.4 M concentration. Both samples also shared a significant increase in optical transmission when exposed to a 0.5 M concentration of acrylic acid, matching the results shown in the transparency spectra for the OC50 sample. The average optical transmission values are displayed in Table 4. 1. The increase in optical transmission for all samples due to the exposure to acrylic acid were confirmed as being statistically significant using the standardised two tier t-test, where the standardised value of probability, $P \leq 0.05$ is adhered to. This suggests that an ITO/PET system exposed to acrylic acid will exhibit a significant increase in optical transmission and it can be seen that the optical properties of the ITO/PET system are dependent upon the ITO layer thickness. This increase in optical transmission is assumed to be a result of a reduction in ITO thickness due to acidic corrosion.

Table 4. 1 Summary of ITO/PET systems mean transparency (%) values in the visible spectrum (400 to 800 nm)

Sample	Reference	0.1 M	0.2 M	0.3 M	0.4 M	0.5 M
OC50	76 ± 1.79	81 ± 1.8	81 ± 0.29	81 ± 0.12	81 ± 1.36	83 ± 2.81
OC100	76 ± 0.41	76 ± 0.35	77 ± 1.44	78 ± 0.76	77 ± 0.35	84 ± 4.66
OC300	84 ± 0.2	84 ± 0.4	84 ± 0.55	85 ± 0.71	85 ± 0.2	88 ± 0.67

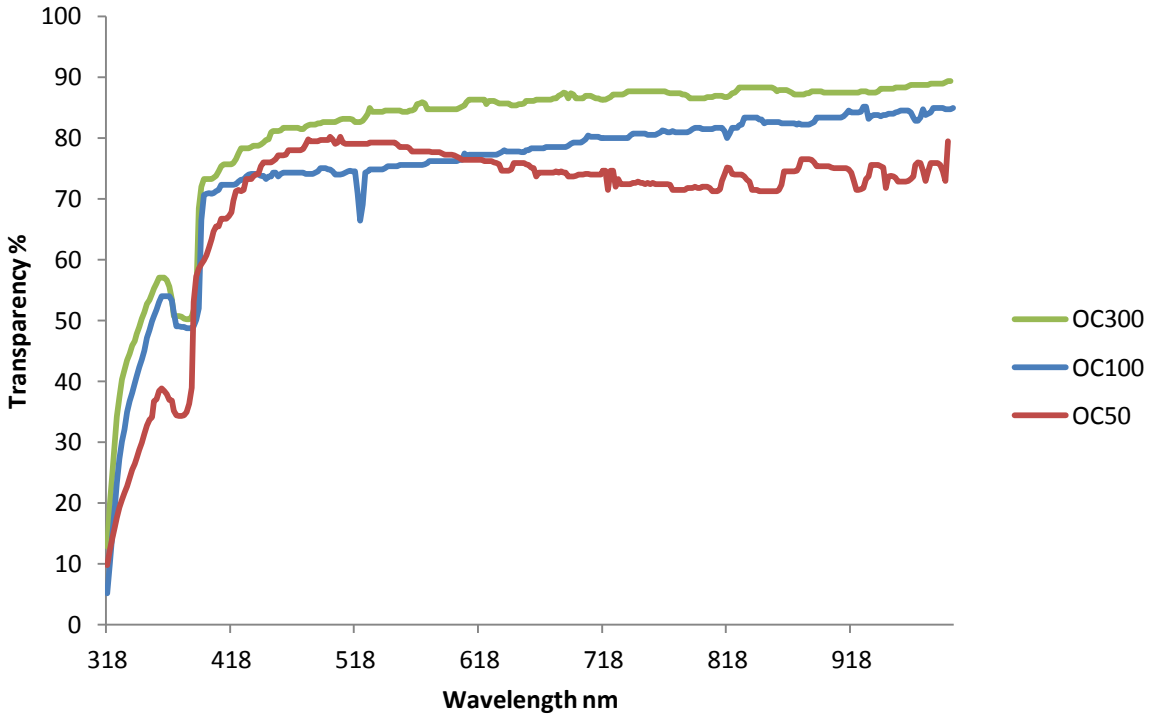

Figure 4. 1 Transparency of OC50, OC100 and OC300 samples exposed to no acid

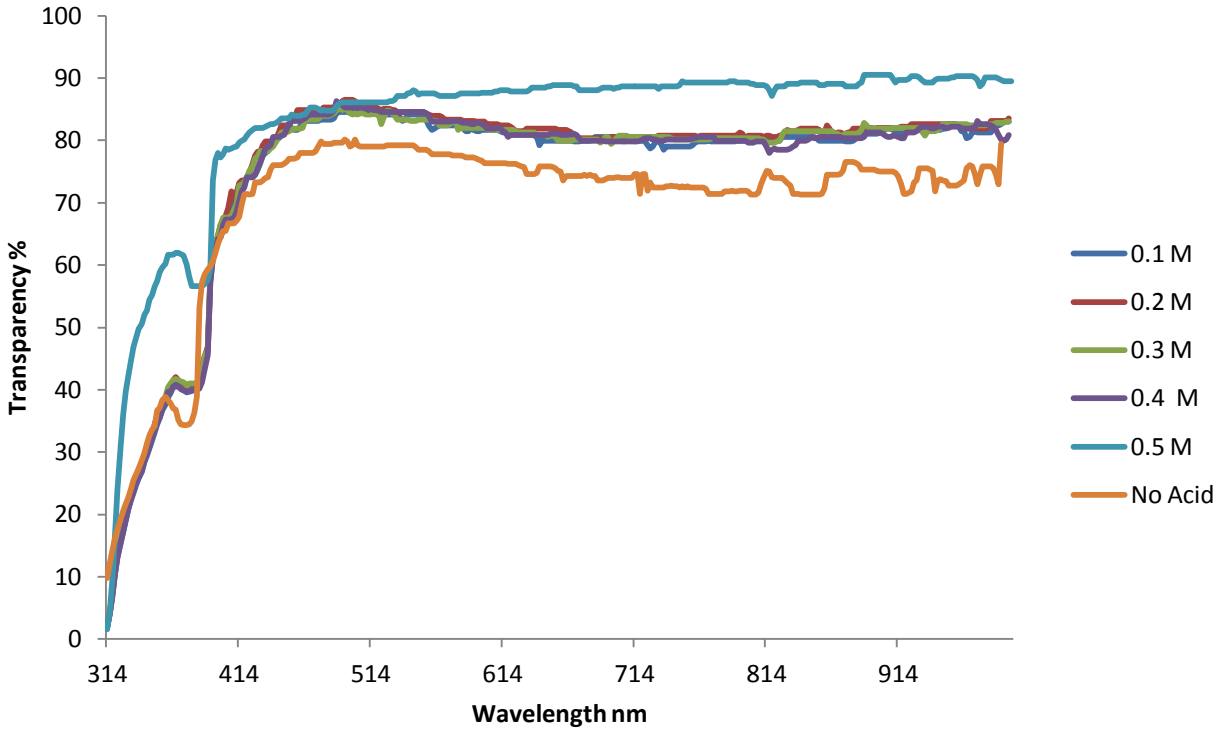

Figure 4. 2 Transparency spectra for OC50 samples exposed to acidic concentrations of 0.1 M to 0.5 M

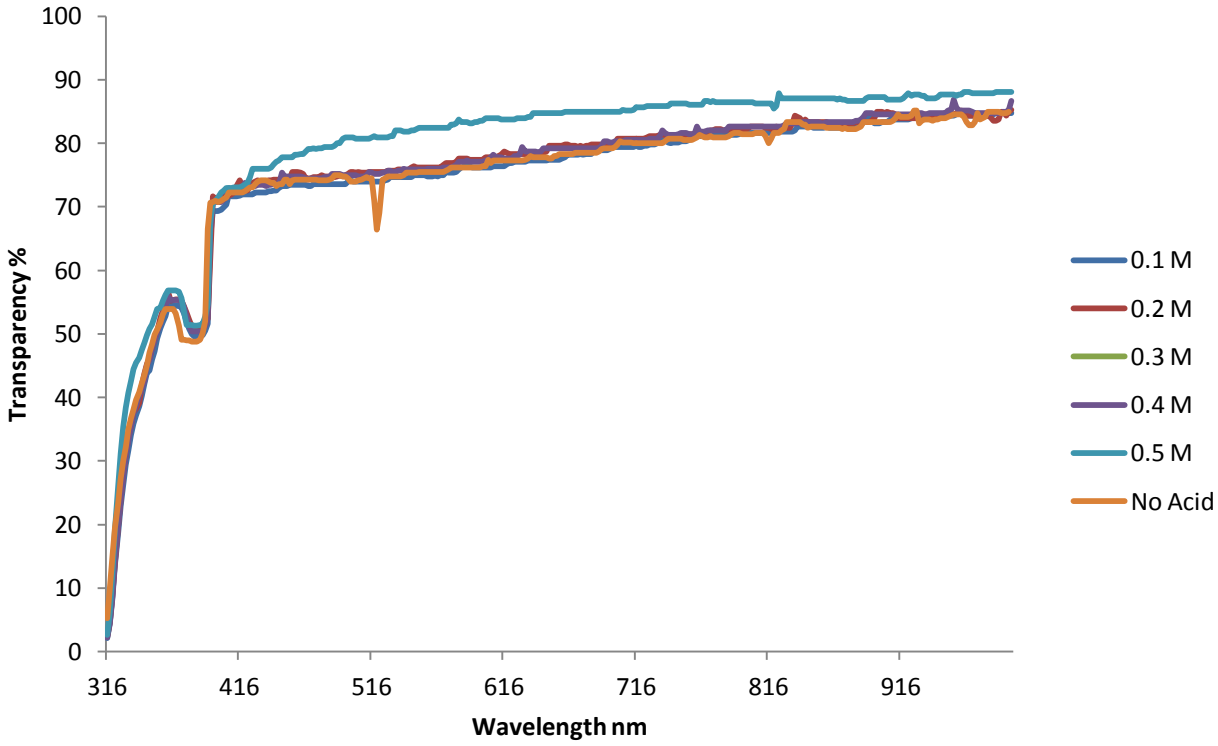

Figure 4. 3 Transparency spectra for OC100 samples exposed to acidic concentrations of 0.1 M to 0.5 M

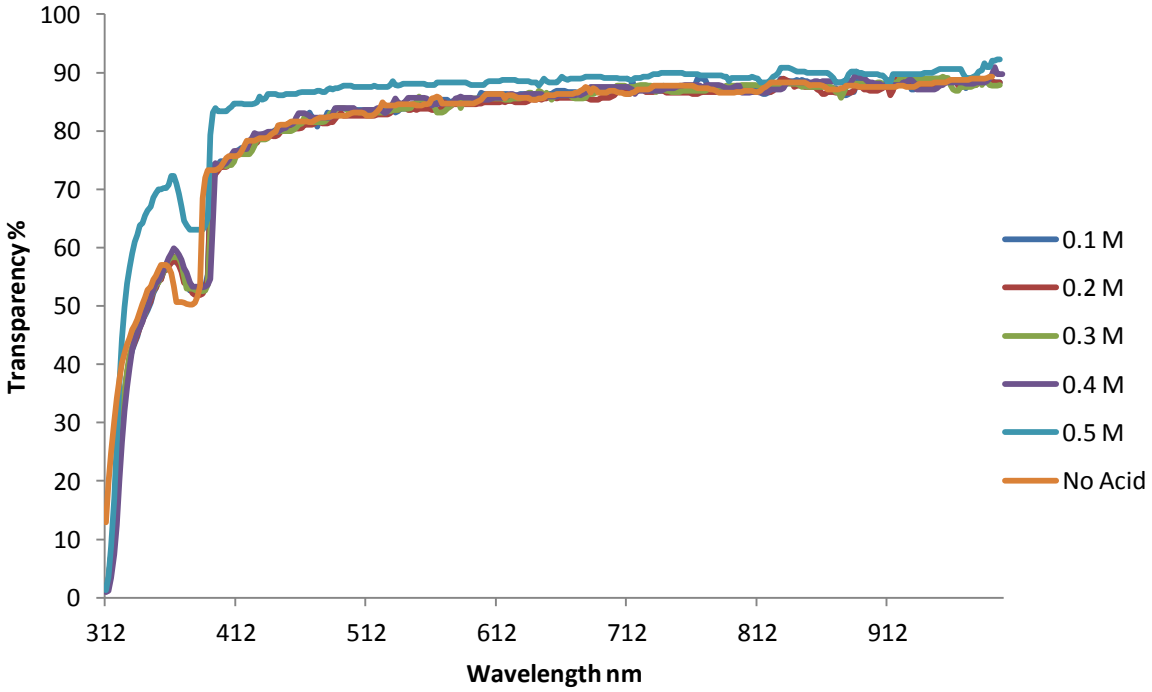

Figure 4. 4 Transparency spectra for OC300 samples exposed to acidic concentrations of 0.1 M to 0.5 M

4.1.2 Electrical resistance

The sheet resistance of the thin film samples in this project were investigated using the four point probe testing method (section 3.2.1). From each of the A4 sample sheets (OC50, OC100 and OC300) 90 29/29 mm square samples were created and tested, 75 of which were placed in 25ml of acrylic acid varying in concentrations from 0.1 M to 0.5 M for two hours whilst 15 were used as reference samples. Due to the variation in sheet resistance over the surface of the samples due to surface flaws, ten measurements were taken and an average sheet resistance for each sample was derived. The mean sheet resistances of the samples can be seen in Table 4. 2.

Table 4. 2 Mean sheet resistances of OC50, OC100 and OC300 samples

Acidic Concentration	OC50 (Ω/□)	OC100 (Ω/□)	OC300 (Ω/□)
No Acid	51.45 ± 0.61	70.56 ± 0.77	312.28 ± 5.10
0.1M	52.72 ± 0.74	73.26 ± 1.64	715.1 ± 333.39
0.2M	54.18 ± 1.13	73.96 ± 2.01	775.25 ± 85.60
0.3M	56.35 ± 1.94	72.74 ± 0.47	1207.08 ± 109.26
0.4M	56.53 ± 0.94	74.64 ± 0.67	1000.27 ± 380.56
0.5M	58.09 ± 1.13	76.81 ± 2.53	1422.6 ± 413.98

As previously stated, the OC50, OC100 and OC300 should exhibit sheet resistances of 50 Ω/□, 100 Ω/□ and 300 Ω/□ respectively according to Solutia Films Inc. Whilst the four point probe confirms this for the OC50 and OC300 samples, it is important to note that the OC100 sample actually exhibits a sheet resistance 70 Ω/□. This could be due to a number of problems during the deposition process such as; a variation in the sputter current, a low applied voltage or a change of pressure within the chamber. It may also indicate a greater thickness of the ITO layer than originally anticipated. The identification of the samples ITO

thickness was attempted using etched samples examined under a profilometer, however due to the samples being commercially manufactured and pre-deposited, this experimental was unable to provide a reliable set of data.

The results displayed in Table 4. 2 initially suggest that the OC50 and OC100 samples sheet resistances are not affected to the same degree as the OC300 sample by the influence of acrylic acid exposure up to 0.5 M. However via the use of the standardised two-tier t-test theses results indicate that exposure to even low concentrations of acrylic acid such as 0.1M, has a statistically significant effect on the ITO/PET systems sheet resistance with average values of $P \leq 0.01$ for both the OC50 and OC100 samples. The OC300 sample displays a more obvious significant change in sheet resistance. It can be seen that even at very low acidic concentrations (0.1 M) the average sheet resistance had shown an increase of over 100%. It is also important to note the extremely high standard deviation values for the OC300 samples, indicating that the influence of acrylic acid does not systematically affect the ITO/PET system, but rather causes random flaws within its sheet resistance. Furthermore, the results show that the electrical properties of these ITO/PET systems are dependent upon the ITO layer thickness. The two-tier t-test confirms the previous results as statistically significant.

4.2 Mechanical properties

4.2.1 Uniaxial tensile testing

The uniaxial tensile test was conducted by using the Instron tensile testing machine at a crosshead speed of 0.08 mm/min. 75 'dumbbell' samples were placed in an acrylic acid solution of 25 ml varying from 0.1 to 0.5 M for five hours and 15 reference samples were not exposed to any acidic environments. The tensile test was conducted with *in situ* monitoring of the samples electrical resistance to evaluate the critical onset strain (COS) at which the ITO/PET systems begin to lose their electrical functionality and to observe any changes in the resistance behaviour after exposure to a range of acrylic acid concentrations.

It can be seen that with an increase in tensile strain the normalised resistance of the ITO/PET system remains constant up to a certain strain percentage, known as the critical onset strain (COS). This strain percentage promotes the onset crack formation within the brittle ITO layer. With a further increase in strain, the normalised resistance gradually increases as a result of crack formation and propagation within the ITO layer. In addition to this, it can be seen that the COS is dependent upon the ITO thickness where the thinner the ITO film, the higher the COS observed at a relative strain percentage.

The electro-mechanical behaviour of the ITO/PET samples (OC50, OC100 and OC300) without exposure to acrylic acid environments can be seen in Figure 4. 5, Figure 4. 6 and Figure 4. 7. These figures indicate a relative COs of 1.3%, 2.3% and 2.1% for the OC50, OC100 and OC300 samples respectively. Analysis of these results indicates that the COs of the ITO film layer shares a relation to the elongation at the yield point of the PET substrate and also indicates that the failure of the ITO film initiates at the onset of plastic deformation

region of the PET substrate. These results conform to the notion that the COS is dependent of the thickness of the ITO film layer. Also it can be noted that the thickness of the ITO layer also affects the modulus of elasticity of the PET substrates, where a thick ITO layer such as the OC50 sample results in a lower modulus of elasticity.

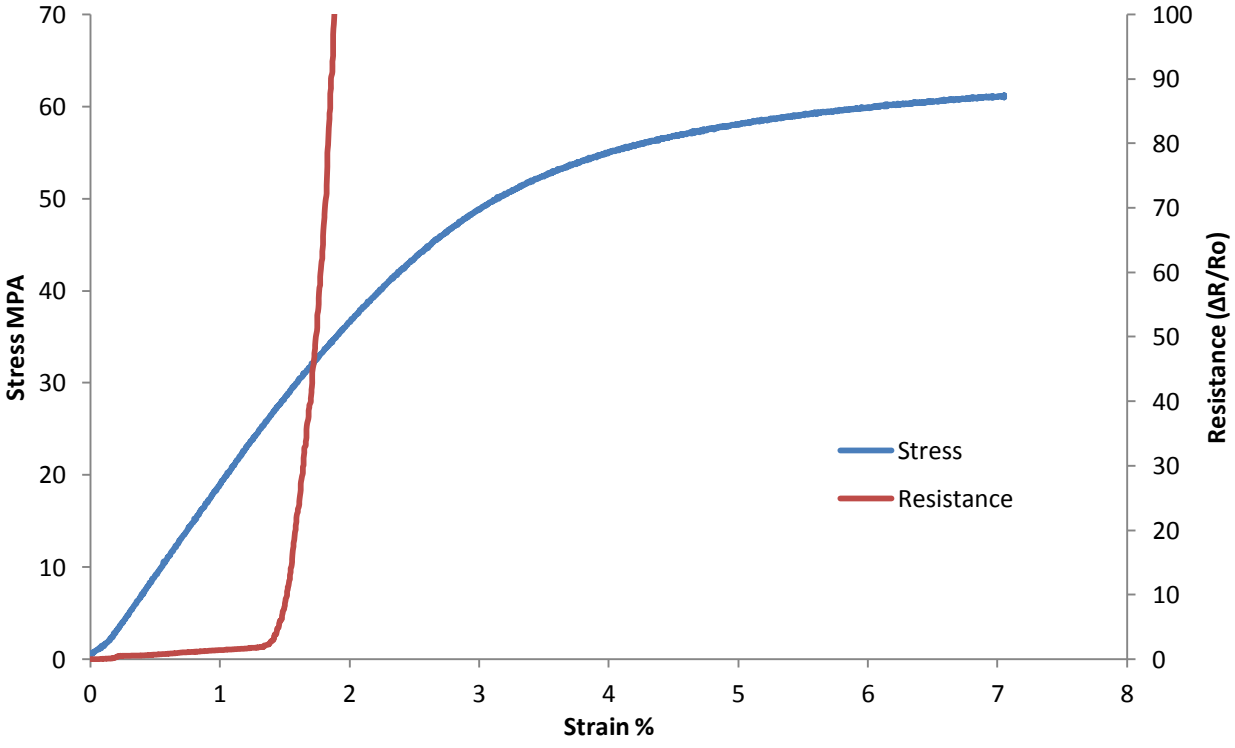

Figure 4. 5 Electro-mechanical behaviour of the OC50 reference sample under uniaxial tensile strain

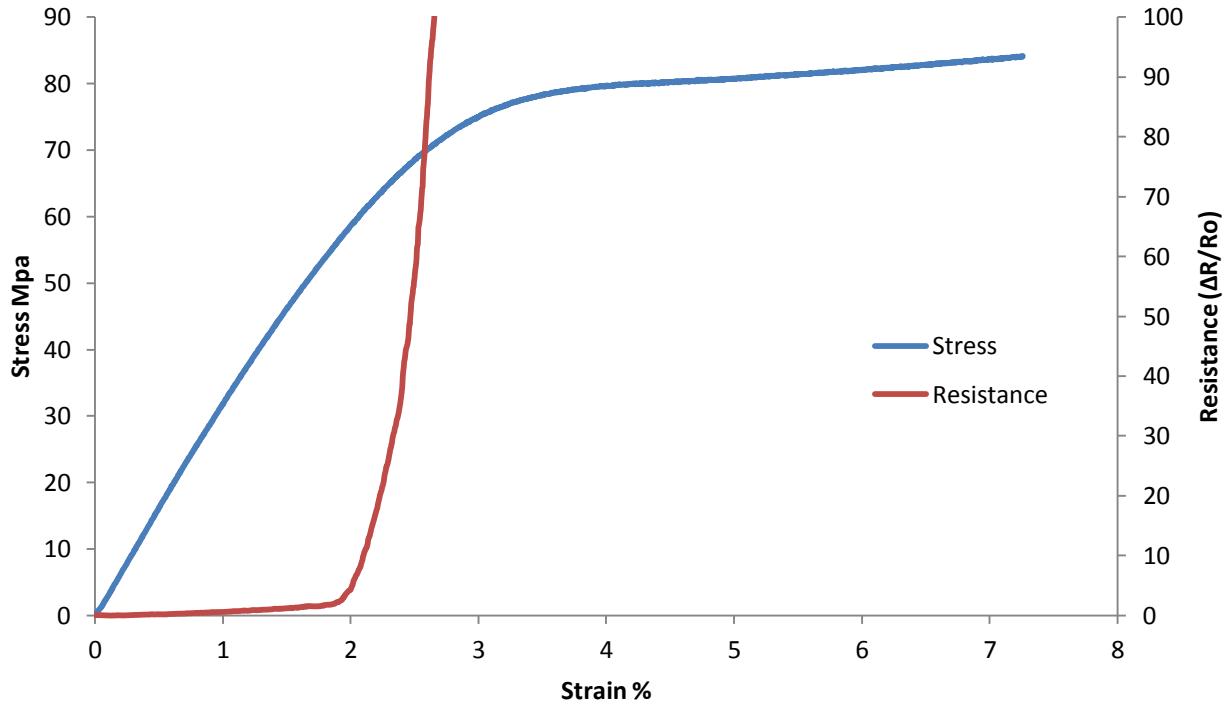

Figure 4. 6 Electro-mechanical behaviour of the OC100 reference sample under uniaxial tensile strain

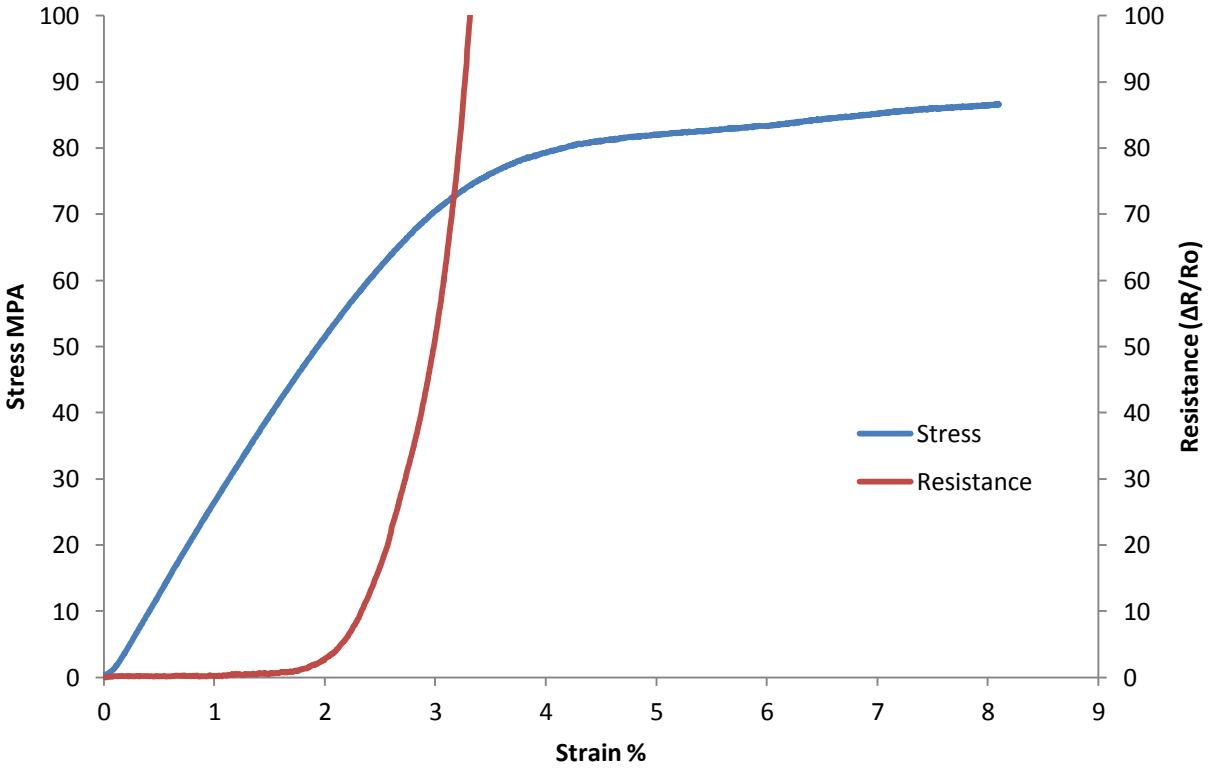

Figure 4. 7 Electro-mechanical behaviour of the OC300 reference sample under uniaxial tensile strain

The effects of acrylic acid on the electro-mechanical properties of these ITO/PET systems were also systematically investigated. Table 4. 3 displays the mean critical onset strain values for all the samples tested in both acidic and non acidic conditions and Figure 4. 9, Figure 4. 10 and Figure 4. 11 display the change in the increment of electrical resistance for the OC50, OC100 and OC300 samples respectively. Previous work (Morris et al., 2008) showed that increasing the acidic concentration resulted in a decrease in the samples ability to resist strain. However it can be seen that these samples displayed fluctuating results. Firstly with regards to the OC50 and OC100 samples, a statistically significant effect was not seen to be present when increasing the acrylic acid concentration from 0.1 M to 0.5 M. Moreover, the data displayed in Table 4. 3 imply that the exposure to acrylic acid has increased the mean critical onset strain for the OC50 sample. For the OC300 sample however, increasing the concentration of acrylic acid above 0.1 M resulted in total film failure as no resistance measurement could be recorded.

At this point it is important to note that this was the first experiment to be investigated and therefore is the only experiment where the samples were exposed to varying acrylic acid concentrations for five hours. After noting no electrical resistance could be monitored above 0.1 M for the OC300 sample, exposure time was reduced to two hours for the remaining experiments. This increased exposure time may be the reason for the fluctuating critical onset strains. Further analysis using SEM showed that the reason for the increased critical onset strains may be due to high corrosion of the ITO layer at the edge of the sample resulting in cracking and delamination. This edge corrosion was seen to form cracks before any strain was induced and was seen to cause delamination at the edge as a result of induced strain.

The Kelly-Tyson cracking model displayed in Figure 4. 8 indicates that at each crack there is non conducting gap between the two sides of the ITO surface, however there is also a small interfacial conducting layer that binds these two sides (Leterrier et al., 1997). The exact composition of this interface is not known, however it is assumed to be a combination of both the ITO layer and the PET substrate. An increase in strain will result in the crack width also increasing, from this further cracks will initiate and propagate and transverse cracks will propagate perpendicular to the load direction. This is assumed to account for the reduction in conductivity and may be masking the point at which the actual critical onset strain takes place, and therefore the increase of the critical onset strains seen, should be disregarded.

It can therefore be seen that exposure to acrylic acid has detrimental effects to these ITO/PET systems. The experiment however also gave supported the notion that exposure to acrylic acid results in a decrease in the ITO/PET systems ability to resist strain as previously claimed (Morris et al., 2008).

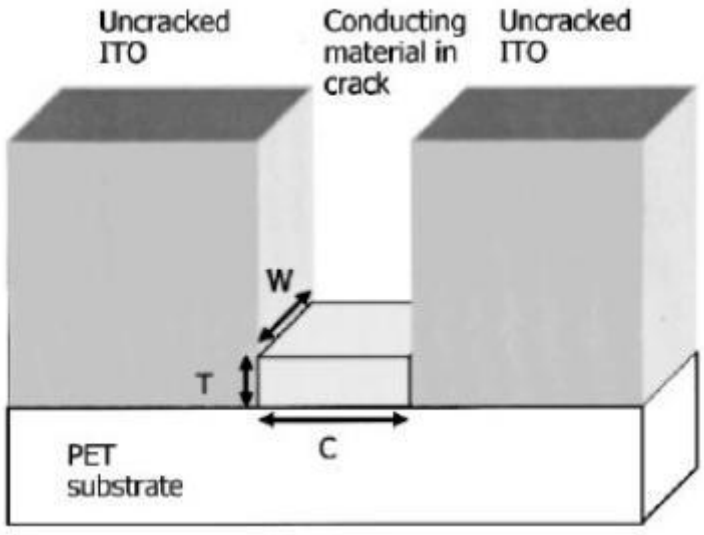

Figure 4. 8 Schematic indicating a thin conductive material bridging ITO crack, adapted from (Cairns et al., 2000).

Table 4. 3 Mean critical onset strains of ITO/PET systems under tensile strain (%)

Sample	Reference	0.1 M	0.2 M	0.3 M	0.4 M	0.5 M
OC50	1.3 ± 0.24	2.9 ± 0.82	2.1 ± 1.25	3.1 ± 0.28	2.6 ± 1.13	2.9 ± 1.16
OC100	2.3 ± 0.33	2.5 ± 1.57	0.36 ± 0.8	1.6 ± 1.48	0.9 ± 1.92	1.9 ± 2.00
OC300	2.1 ± 0.20	2.6 ± 0.98	NA	NA	NA	NA

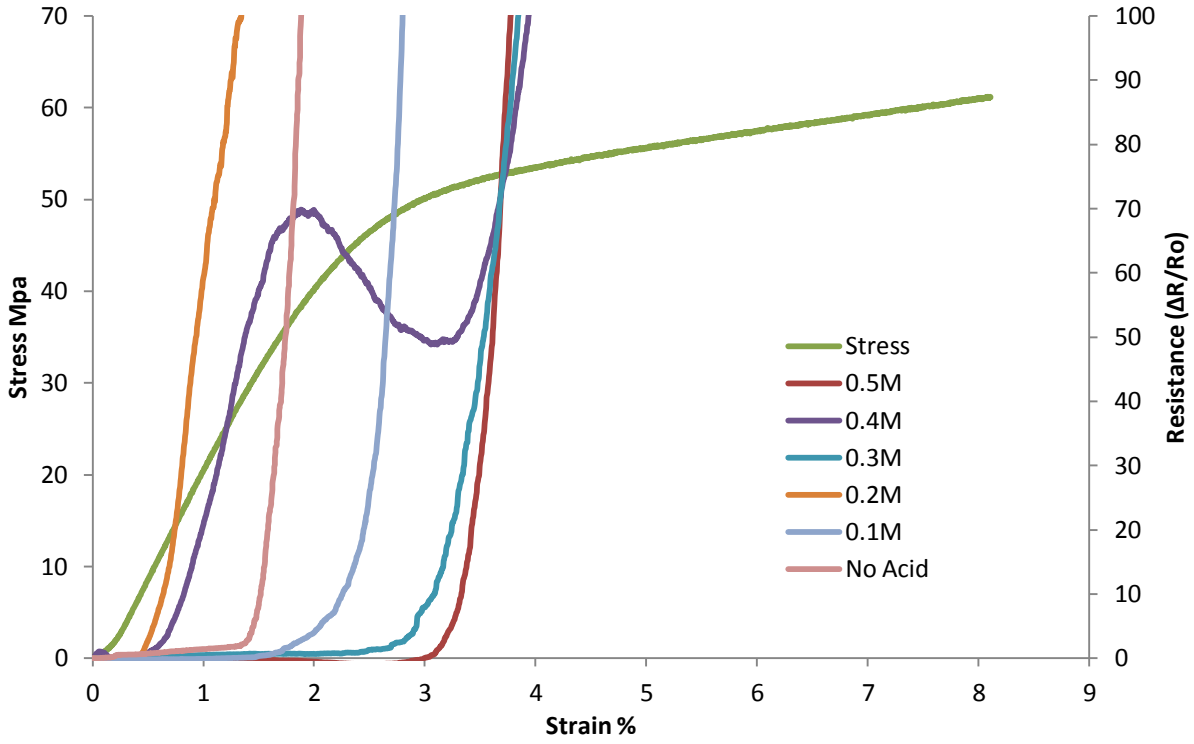

Figure 4. 9 Electro-mechanical behaviour of the OC50 sample after exposure to differing concentrations of acrylic acid (no-acid to 0.5 M) under uniaxial tensile strain

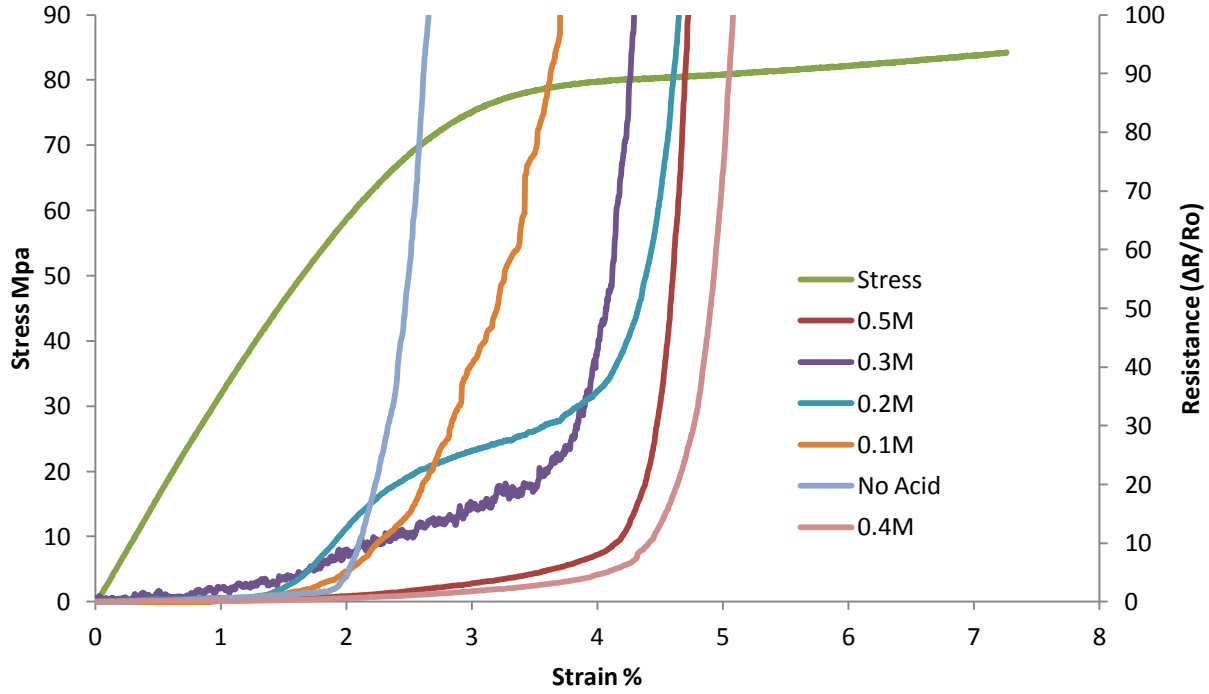

Figure 4. 10 Electro-mechanical behaviour of the OC100 sample after exposure to differing concentrations of acrylic acid (no-acid to 0.5 M) under uniaxial tensile strain

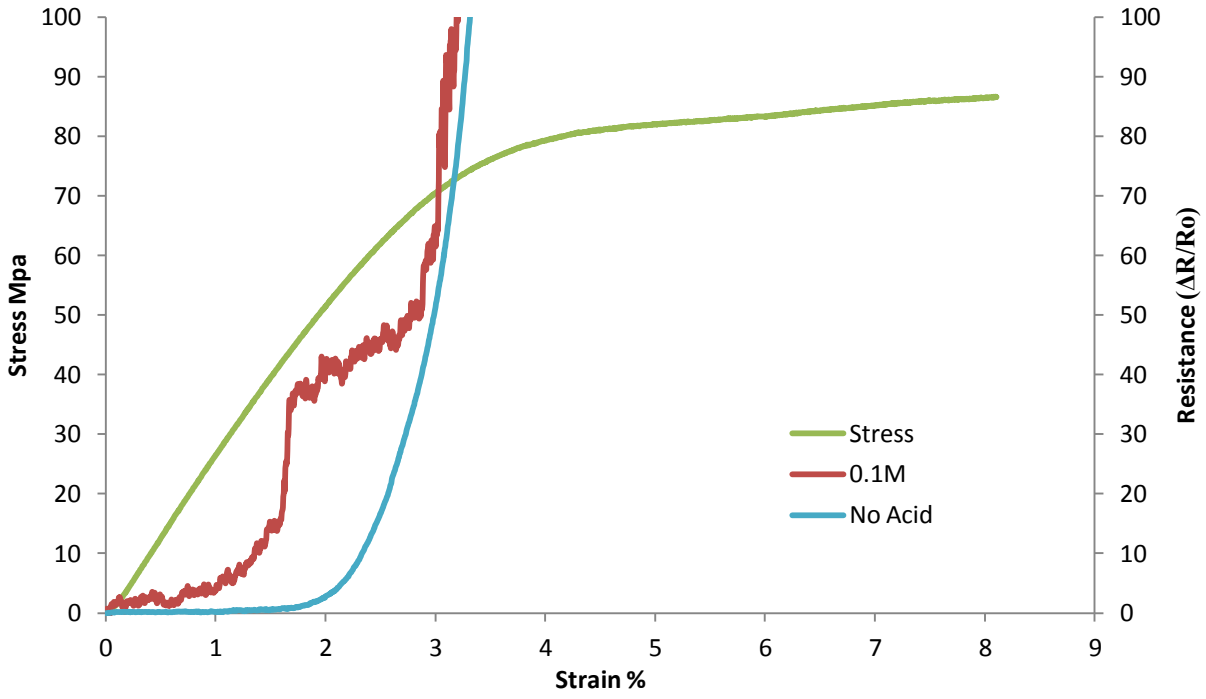

Figure 4. 11 Electro-mechanical behaviour of the OC300 sample after exposure to differing concentrations of acrylic acid (no-acid to 0.5 M) under uniaxial tensile strain

4.2.2 Monotonic bending

Monotonic bending of the ITO/PET thin film samples was conducted using a device that was designed and developed by Grzegorz Potoczny (Potoczny, 2011) which has been previously discussed in section 3.2.4. 75 'dumbbell' samples were placed in an acrylic acid solution of 25ml varying from 0.1 to 0.5M for two hours and 15 reference samples were not exposed to any acidic environments. The experiment was performed in order to investigate the flexibility characteristics of ITO/PET thin films whilst being subjected to tensile and compressive stresses. The influence of acrylic acid on the flexibility characteristics of these samples has also been investigated.

4.2.2.1 Monotonic bending under tensile stress

The monotonic bending experiment enables analysis of the increment of resistance as a function of radius of bending curvature and can be seen in Figure 4. 12. The results showed that with a decrease in the radius of curvature, the electrical resistance displayed a sudden increase at a critical radius point, exhibiting a similar resistance failure curve of that seen in tensile tests when the COR is reached and is due to crack formation and propagation in the ITO layer.

During monotonic bending whilst the sample is under tensile stress, conductive failure occurs at around 5, 5.6 and 2.3mm for the OC50, OC100 and OC300 samples respectively. As previously discussed the samples have differing ITO layer thicknesses, the thickest of which is the OC50 sample (OC100 sample shares a similar ITO thickness), where the thinnest layer is seen within the OC300 sample. Therefore, during monotonic bending under tensile stress, it can be seen that ITO/PET systems with thin ITO layers display a greater degree of flexibility that that of ITO/PET systems with a thick ITO layer. With this in mind it can be

said that during monotonic bending under tensile stress, the mechanical properties of the ITO/PET systems are dependent on the ITO film thickness.

After exposure to varying concentrations of acrylic acid it can be seen that the degree of flexibility is negatively affected for all samples and an example of which can be seen in Figure 4. 13. Even at low concentrations such as 0.1M, the average critical onset radius (COR) had dramatically increased from 5.6mm ±0.1 to 18.6mm ±5.11 for the OC100 sample and from 2.3mm ±1.23 to 18mm ±10.63 for the OC300 sample. The data for these results has been validated as a significant statistical increase using the two tiered t-test where the standardised value of probability, $P \leq 0.05$ is adhered to. The OC100 and OC300 samples exhibited values of $P \leq 0.002$ and $P \leq 0.05$ respectively. It can also be noted from Table 4. 4, that although the exposure to acrylic acid has resulted in a significant decrease in the degree of flexibility for all samples, the effects do not seem to be dependent upon the acidic concentration. Moreover this suggests that alone acidic corrosion is not the sole cause for failure, it does however facilitate failure. Therefore it can be seen that stress-corrosion cracking is the primary failure mechanism exhibited.

Table 4. 4 Average values of the critical radius of curvature (mm) for ITO/PET systems shown in both acidic and non-acidic conditions under tensile stress.

Sample	Reference	0.1 M	0.2 M	0.3 M	0.4 M	0.5 M
OC50	5±1.49	6.7±5.92	13.3±7.15	16.6±9.96	26±31.62	13.5±3.56
OC100	5.6±0.1	18.6±5.11	7.8±2.66	22.8±15.5	7±5.31	22.03±12.76
OC300	2.3±1.23	18±10.63	5.8±2.2	5±2.96	4±1.96	4±3.04

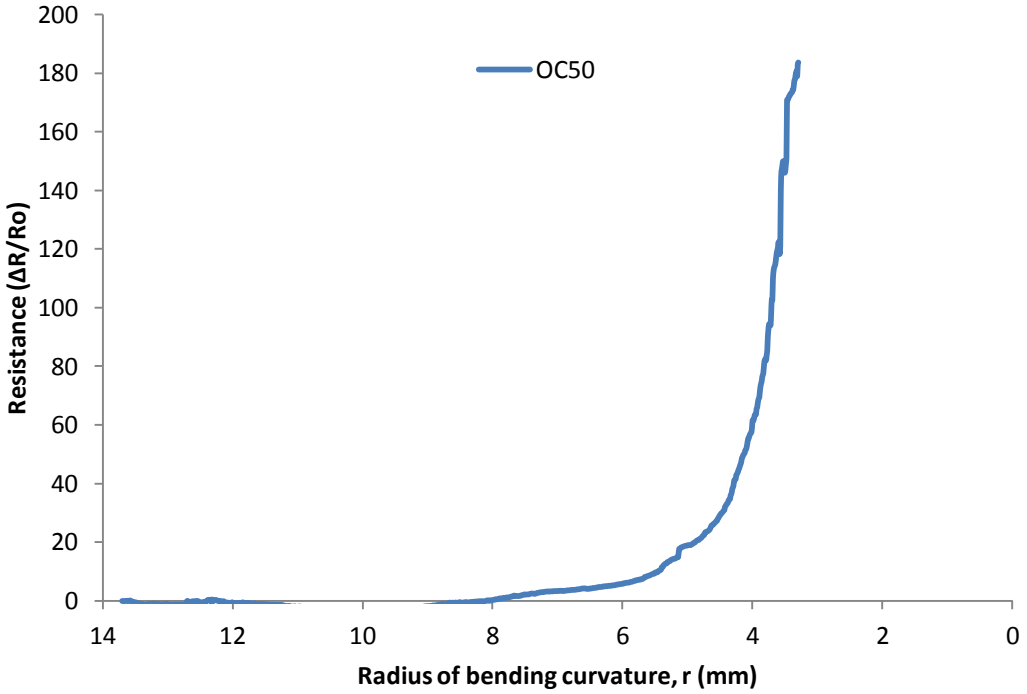

Figure 4. 12 Increase in resistance as a function of radius of bending curvature for the OC50 sample flexed in tension.

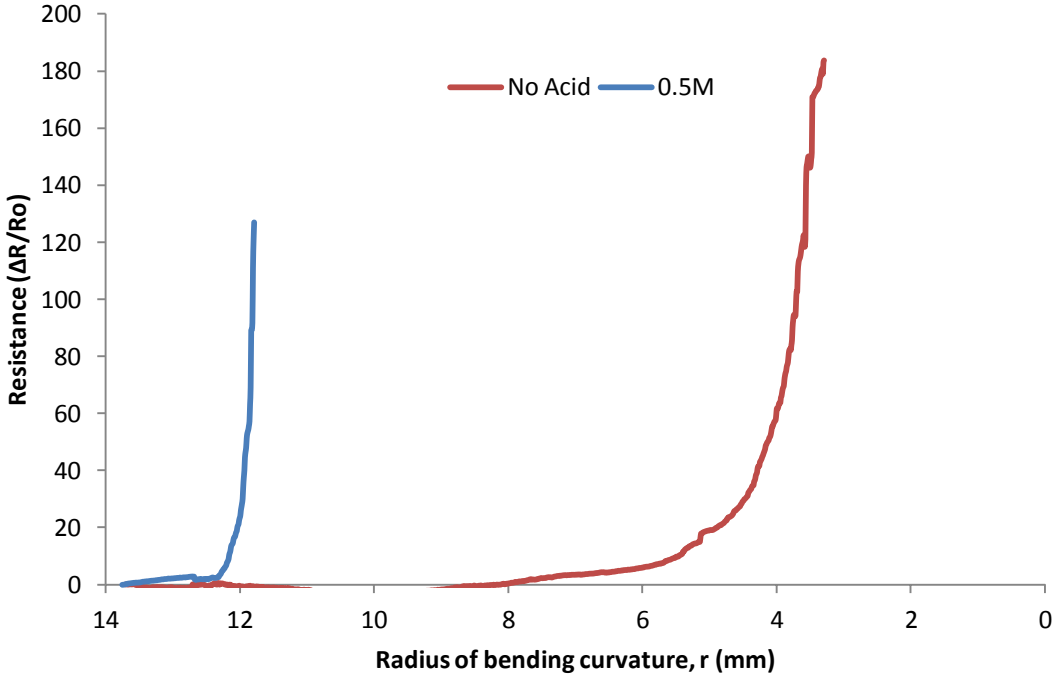

Figure 4. 13 The effect of acrylic acid on the increment of resistance as a function of radius of bending curvature for the OC50 sample flexed in tension.

4.2.2.2 Monotonic bending under compressive stress

Compared to the samples tested under tension, the ITO/PET systems examined under compressive loads show low critical radius of curvature values in the vicinity of 2mm for all samples. Post critical radius the increment of resistance sharply increases in the same manner as the samples examined under tension. The samples do however display a small decrease in resistance prior to the critical onset radius being met and can be seen in Figure 4. 14. The reason for the reduction in resistance may be that; due to the sample being compressed, the distance between the grains within the ITO film will become reduced, this in turn will result in a reduction of possible physical barriers and facilitate the mobility of electrons. Therefore it can be stated that ITO/PET systems that are flexed in compression display a greater degree of flexibility than if they were flexed in tension. A contributing factor to this may be due to the fact that; when samples are flexed in tension, the mechanical properties of the ITO layer are greatly affected by surface flaws such as poor surface roughness, residual stress, sub-microscopic cracks and poor adhesion between the ITO and the PET substrate. However when the sample is flexed in compression, these flaws and cracks are pushed together rather than being forced apart. This suggests that samples in flexed compressive conditions are determined via both the ITO and PET materials intrinsic properties, where as in tension they are determined by the defects present and the thickness of the ITO layer.

Furthermore it can be seen from Figure 4. 14 and Table 4. 5 that unlike the samples tested in tension, exposure to acrylic acid does not have any significant effect on the degree of flexibility for the ITO/PET systems examined in compression. Whilst it was noted that under tension exposure to acrylic acid was a contributory factor for failure, Figure 4. 14 indicates that when flexed in compression even at high acidic concentrations such as 0.5M no

significant effect could be seen. The data for these results have been validated to show no significant statistical change using the two tiered t-test where the standardised value of probability, $P \leq 0.05$ is adhered to. No sample examined in compression issued a standardised probability value of $P \leq 0.05$. This confirms that unlike when the samples are subjected to tension where stress-corrosion cracking is the primary failure mechanism, during compression electro-mechanical failure is dependent upon the intrinsic material properties of the ITO/PET system.

Table 4. 5 Average values of the critical radius of curvature (mm) for ITO/PET systems shown in both acidic and non acidic conditions under compressive stress.

Sample	Reference	0.1 M	0.2 M	0.3 M	0.4 M	0.5 M
OC50	2.1±0.22	2.6±0.77	2.1±0.28	2.1±0.31	2.7±1.88	2.5±1.21
OC100	2.7±3.07	2.4±1.62	2.3±1.48	4.9±5.08	2.4±0.57	2.9±3.10
OC300	1.8±1.11	1.2±1.06	2.2±3.7	1.3±1.21	2.3±1.69	1.9±1.89

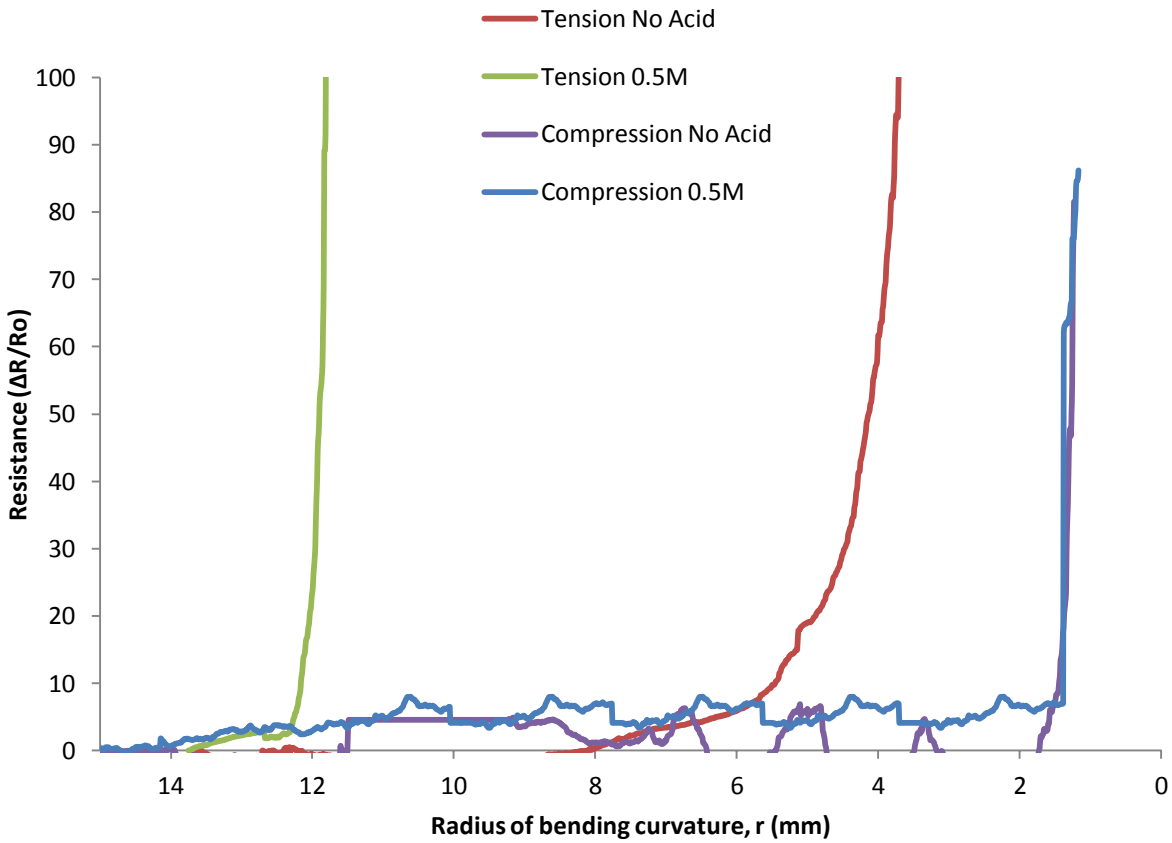

Figure 4. 14 The effect of acrylic acid on the increment of resistance as a function of radius of bending curvature for the OC50 sample flexed in both compression and tension.

4.2.3 Tribological properties

The tribological properties of these ITO/PET systems were investigated via the use of a reciprocating wear test with a mean Hertzian contact pressure of 0.32MPa. The test was conducted after adding a number of customizations to a High Frequency Reciprocating Rig (HFRR), details of which can be seen in section 3.2.5. A total of 45 'dumbbell' samples were placed in an acrylic acid solution of 25ml varying from 0.1 to 0.5M for two hours and nine reference samples were not exposed to any acidic environments. The experiment was conducted with *in – situ* monitoring of the samples electrical resistance to evaluate the point at which the ITO/PET systems begin to lose their electrical functionality. It is important to note at this stage that; due to the structure of the ITO/PET system consisting of a hard brittle layer deposited onto a soft polymer substrate, there is a resulting high modulus mismatch, meaning the response of the polymer substrate during contact cannot be ignored, as is the case with commonly used rigid substrates such as glass. Therefore this experimental technique cannot be used to obtain the mechanical properties of the ITO layer nor does it replicate typical user interaction such as a finger swipe. It does however enable one to develop the understanding of the wear failure mechanisms involved during reciprocating motions that may be found in future manufacturing processes, more so than what can be found with a traditional stylus technique and the effects, if any, that exposure to acrylic acid environments may have on the next generation of flexible thin film devices.

An optical microscope is connected to the HFRR and allows immediate *ex-situ* surface analysis of both the ITO/PET sample and also the PTFE ball. From the optical micrographs taken it can be seen that the wear scar displayed on the ITO/PET sample correlates with the wear scar shown on the PTFE ball, as shown in Figure 4. 15. From these micrographs we can

also notice a difference in the area of these wear scars, where; the ITO/PET sample displays a smaller affected area (575 μm) than the affected wear area of the PTFE ball (603 μm). This indicates that although of the PTFE ball is in contact with the surface of the sample, only a certain part within the area of contact contributes to the formation of a wear scar.

Further analysis of these micrographs coupled with the change in the samples electrical conductivity, indicates the possible wear mechanisms of ITO/PET systems. Traditionally, electro-mechanical failure of the ITO layer has been determined by a critical point at where there is a noticeable 10% increase in the increment of electrical resistance ($\Delta R/Ro$), such as critical onset strain (Cairns et al., 2000). However, Figure 4. 17 to Figure 4. 22 display both the optical micrographs and the number of cycles to failure for all three samples (OC50, OC100 and OC300). It can be seen that crack formation and propagation occurs before a 10% increase in the increment of resistance, with some samples displaying the start of critical failure at increases as low as 0.40%. This is due to the wear interaction of the PTFE ball with the ITO surface. In this experiment, the reciprocating motion did not span the entire width of the sample (edge to edge). The reciprocating motion only occurred in the middle of sample, resulting in crack initiation and propagation from the wear site perpendicular to the wear direction. Due to the wear in this centralised location micrographs indicated that only the part of the sample subjected to wear exhibited crack formation and propagation, resulting in the sample displaying affected and non affected regions as shown in Figure 4. 16. The resulting resistance graphs shown in Figure 4. 20, Figure 4. 21 and Figure 4. 22 correlate to this notion of differing affected regions within the sample. The resistance graphs indicate an increase in electrical resistance, followed by levelling off to a plateau.

This is due to the sample working as a simple parallel circuit and can be explained via equation 4.1.

$$\frac{1}{R_{total}} = \frac{1}{R_{damaged}} + \frac{1}{R_{undameged}} \quad (4.1)$$

The flow of electrons through the sample is affected by crack formation and results in a small increase in electrical resistance; as crack propagation occurs due to continued wear, catastrophic failure can be observed within the affected region where electrical resistance reaches infinity, the recorded resistance from this point is then monitored via the unaffected region. Therefore the normalised indication of electro-mechanical failure by an increase in electrical resistance of 10% cannot be applied here.

The start of critical failure within the damaged region for all samples (OC50, OC100 and OC300) was analyzed. The results showed that; the OC50 samples critical failure occurred at around 500 cycles before exposure to acrylic acid solutions, OC100 reached failure at around 220 cycles and the OC300 sample accomplished around 570 cycles before reaching critical failure within the affected region. After acrylic acid exposure a decrease in the number of cycles for all samples was observed. Even at concentrations as low as 0.1M, the OC50 sample's cycles to failure was reduced from 500 cycles to 250 cycles and the OC300 sample was reduced from 570 cycles to 200 cycles. The OC100 sample showed a reduction from 220 cycles to around 200 cycles when exposed to an acrylic acid concentration of 0.2M. Increasing the concentration of acrylic acid was not seen to have a significant effect on the number of cycles that critical failure started to occur in the affected region. At high concentrations of 0.5M the number of cycles to failure was found to be around; 215, 190 and 195 cycles to failure for the OC50, OC100 and OC300 samples respectively. This implies

that acrylic acid exposure is not the cause for failure, moreover it merely facilitates the wear failure mechanism. It was also noticed that past this initial critical failure point within the affected region, exposure to any acrylic acid solutions resulted in a large increase in the increment of resistance shown. For the OC50 and OC100 samples, the increases shown were similar for all samples up to 0.4 M, and at 0.5 M an even greater increase was seen. For the OC300, all acidic concentrations caused a high, non uniform increase in resistance. This indicates that the acrylic acid exposure affects the unaffected region as well as facilitating failure via stress corrosion cracking within the affected region. Furthermore the optical micrographs of the OC300 samples show more prominent wear scars than those of the OC50 and OC100 samples that contain a thicker ITO layer, indicating that the degree of wear is dependent on the ITO film thickness.

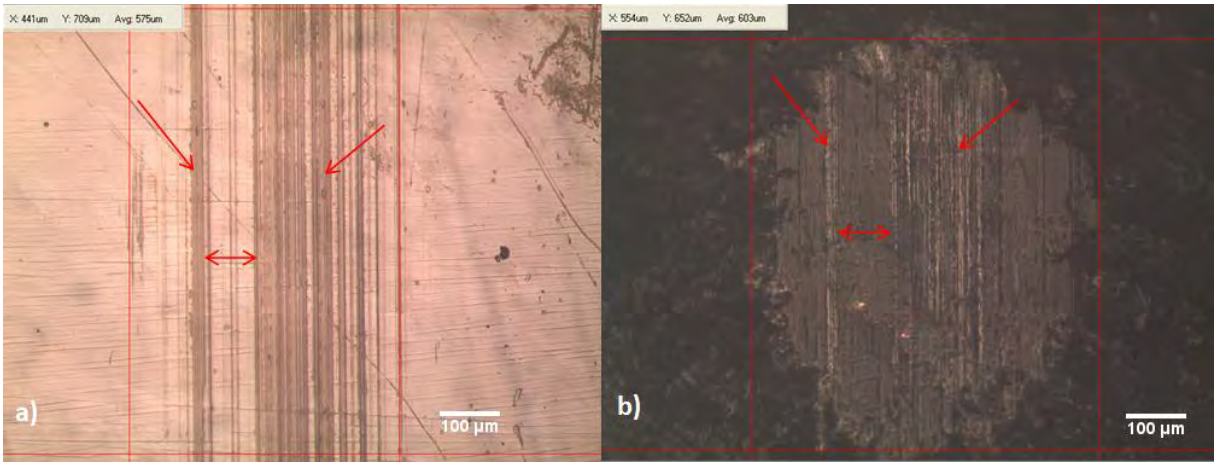

Figure 4. 15 *Ex situ* optical micrographs displaying the wear scar on both the ITO/PET sample and the PTFE ball. The red lines show the area of the wear scar and the red arrows indicate matching wear features on a) ITO/PET sample and b) PTFE ball

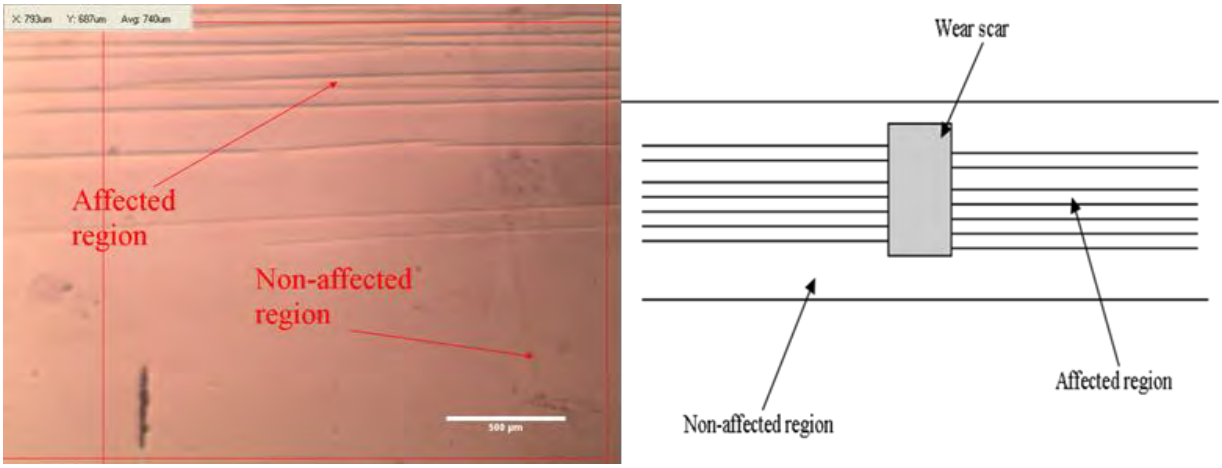

Figure 4. 16 Optical micrograph and schematic diagram indicating affected regions of the sample

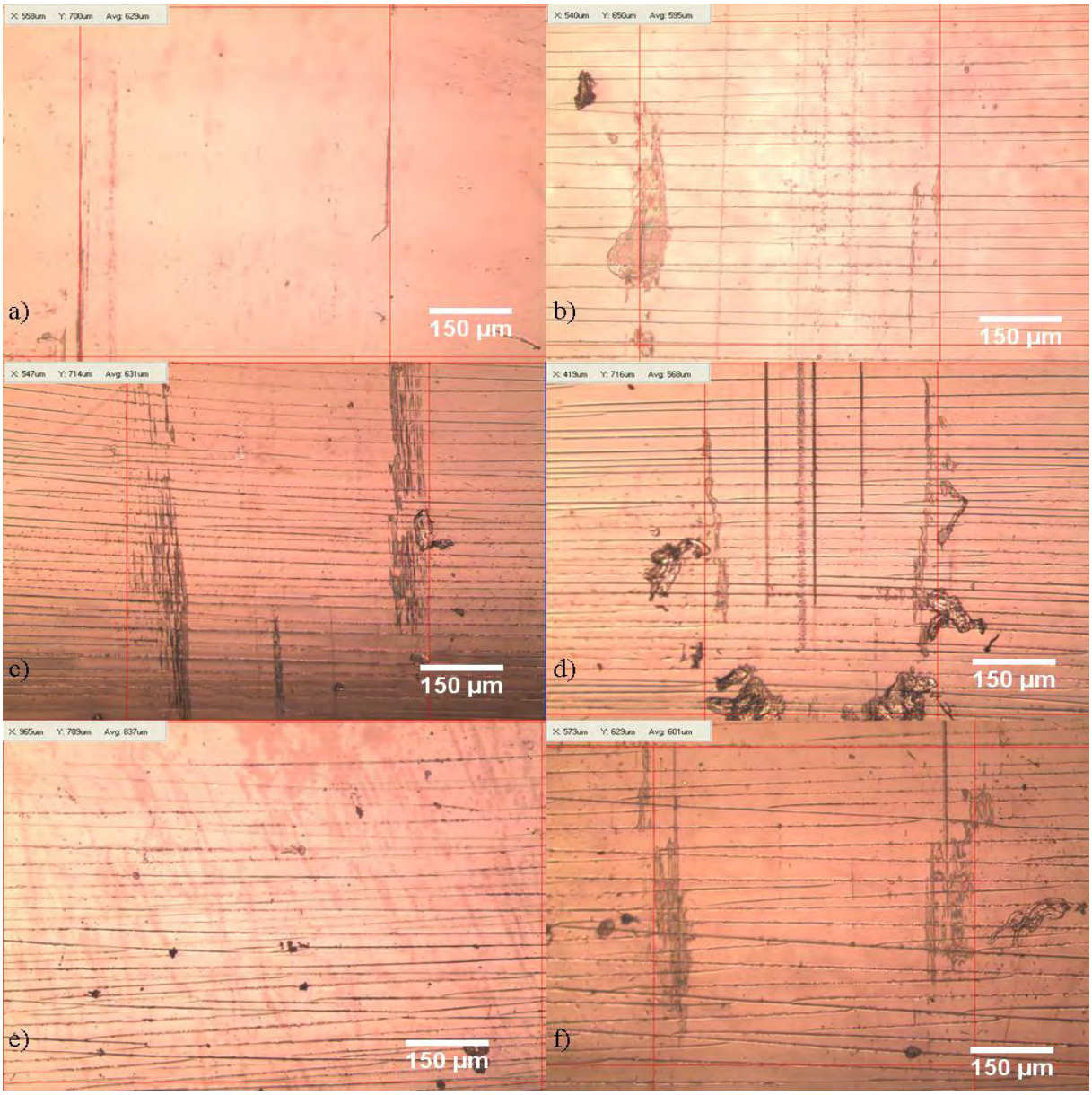

Figure 4. 17 *Ex situ* optical micrographs presenting the wear scars and crack formation for the OC50 sample exposed to an acrylic acid solution for two hours at; a) no acid, b) 0.1 M, c) 0.2 M, d) 0.3 M, e) 0.4 M, f) 0.5 M.

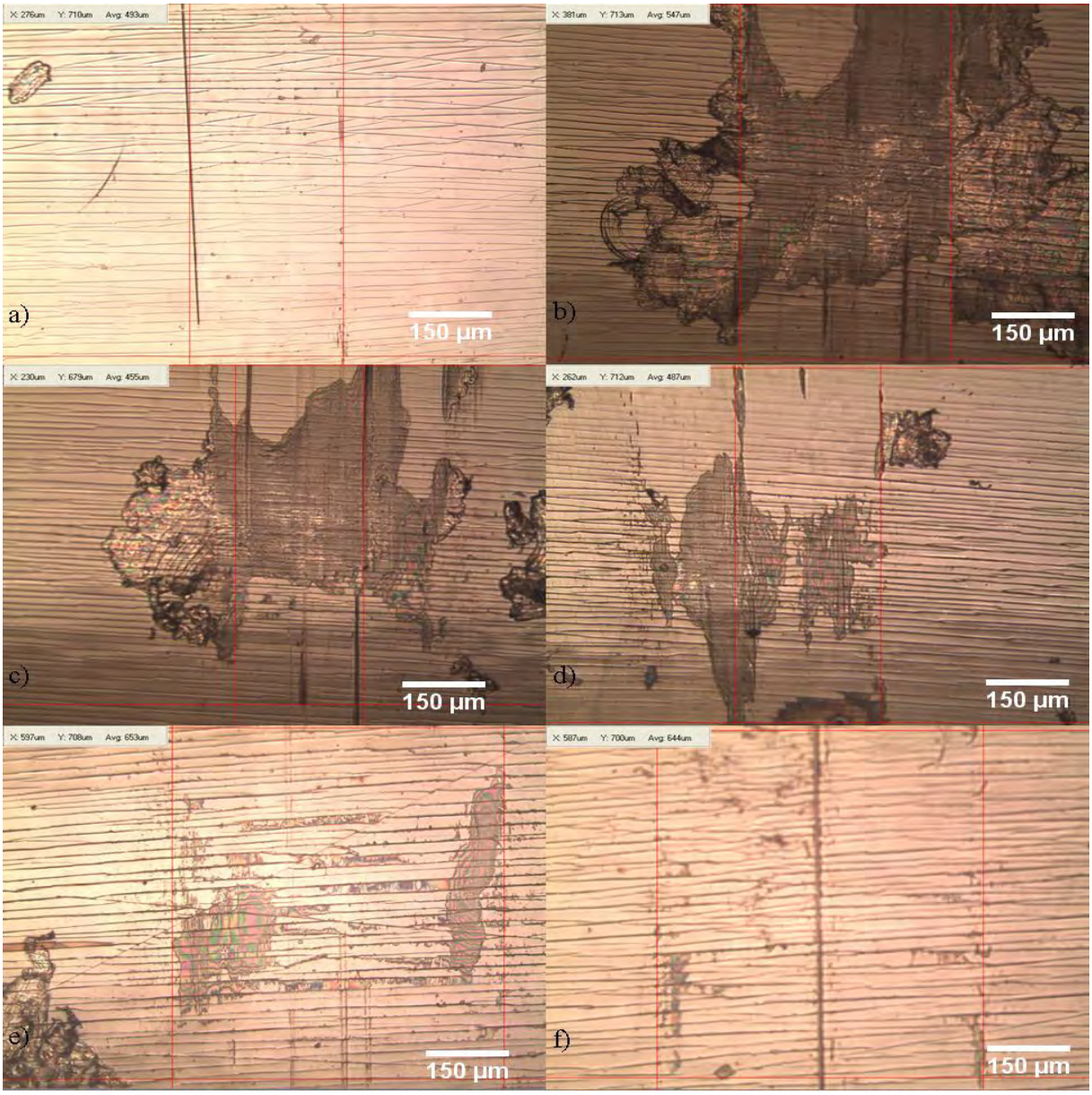

Figure 4. 18 *Ex situ* optical micrographs presenting the wear scars and crack formation for the OC100 sample exposed to an acrylic acid solution for two hours at; a) no acid, b) 0.1 M, c) 0.2 M, d) 0.3 M, e) 0.4 M, f) 0.5 M.

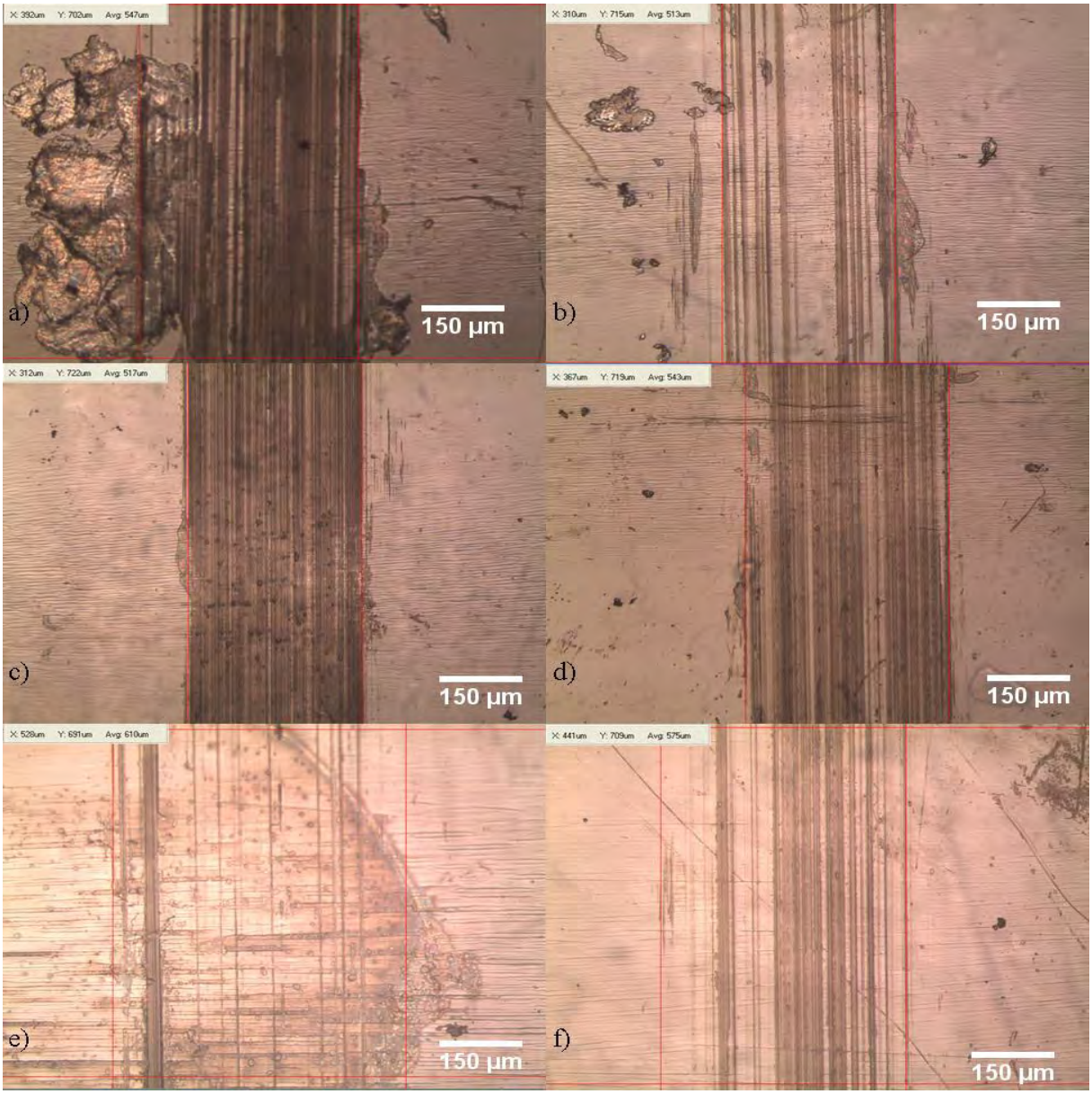

Figure 4. 19 *Ex situ* optical micrographs presenting the wear scars and crack formation for the OC300 sample exposed to an acrylic acid solution for two hours at; a) no acid, b) 0.1 M, c) 0.2 M, d) 0.3 M, e) 0.4 M, f) 0.5 M.

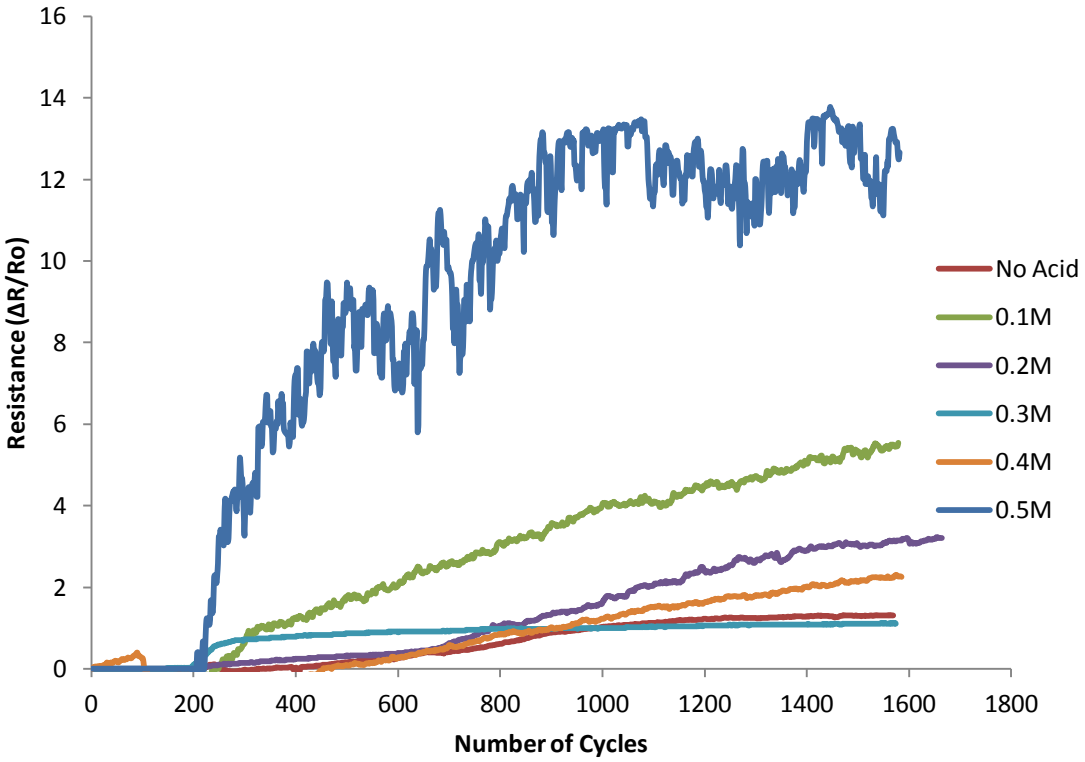

Figure 4. 20 Number of cycles to failure for the OC50 sample up to an acrylic acid solution of 0.5 M.

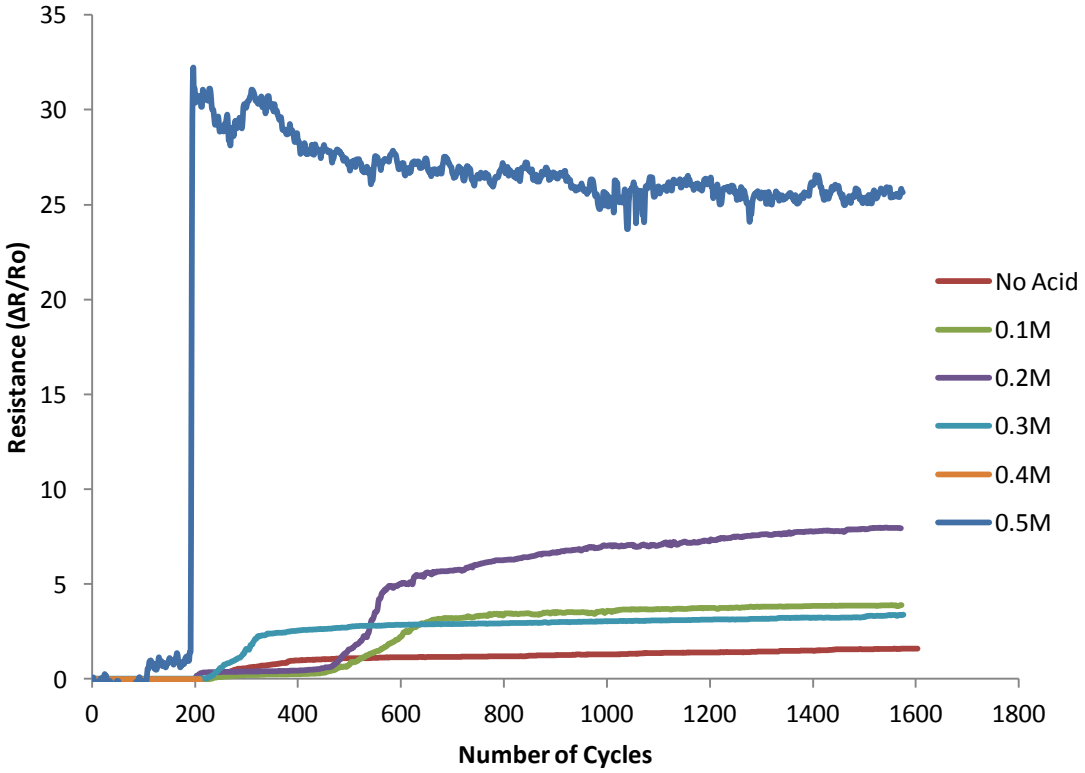

Figure 4. 21 Number of cycles to failure for the OC100 sample up to an acrylic acid solution of 0.5 M.

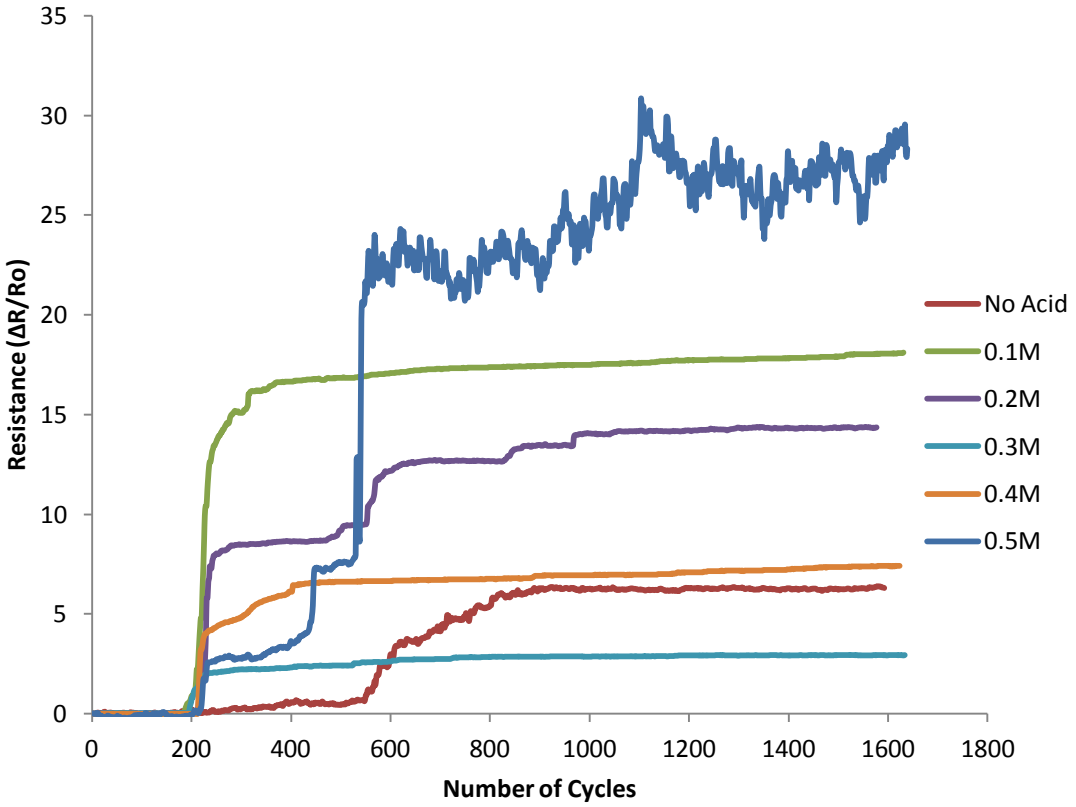

Figure 4. 22 Number of cycles to failure for the OC300 sample up to an acrylic acid solution of 0.5 M

4.3 Surface analysis

4.3.1 ITO surface investigation after acrylic acid exposure

Surface analysis of the ITO layer was conducted using a conventional Joel 6060 SEM before and post acrylic acid exposure to investigate any surface changes due to corrosion prior to any experiments had taking place. Figure 4. 23 displays SEM micrographs of the OC50 sample prior and post acrylic acid exposure at a concentration of 0.1 M. It can be seen that even at low acidic concentrations, corrosion takes place via acidic spot formation. These corrosion spots may form crack initiation sites on the ITO layer and result in a reduction of the electro-mechanical properties of the ITO/PET system.

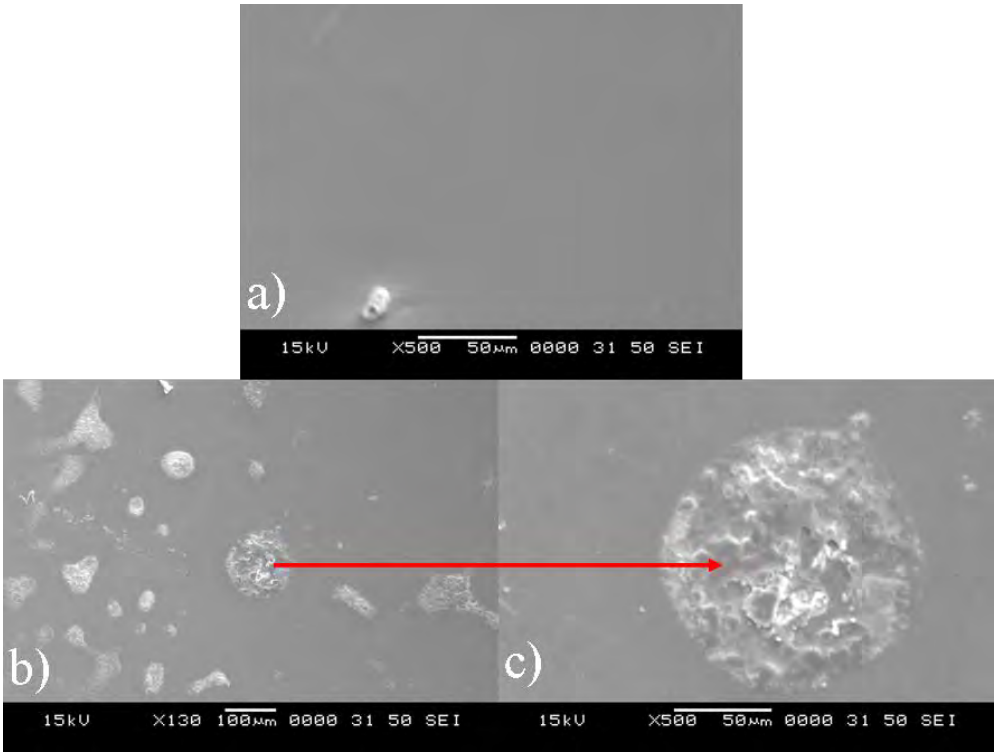

Figure 4. 23 SEM micrographs of indicating acidic corrosion at a) no acid, b) and c) 0.1 M for two hours.

4.3.2 Ex situ SEM investigation after uniaxial tensile testing

All samples were investigated after uniaxial tensile testing using the SEM technique to reveal details of the ITO/PET systems failure mechanisms. The following micrographs display samples that were strained to ~ 8%. Channel cracking of the ITO layer is evident which are parallel to one another and perpendicular to the load direction, which is consistent with previous research.

As previously discussed in section 4.2.1, exposure to acrylic acid can result in corrosive attacks at the edge of the ITO/PET system and can lead to misleading critical onset strains. Evidence of this can be seen in the SEM micrographs displayed in Figure 4. 24 where corrosion is clearly displayed by the black arrow. These micrographs show the ITO/PET system pre and post uniaxial tensile testing. It can be seen that corrosion has taken place at the edge of the sample and small cracks have already began to form prior to any induced strain. After tensile testing large degrees of cracking and delamination can be seen as shown by the red arrow in a sample that inferred it was able to resist strain to a higher degree to that of its reference counterpart. This failure mechanism was not seen however in any of the samples that exhibited decreased critical onset strains due to the exposure of acrylic acid.

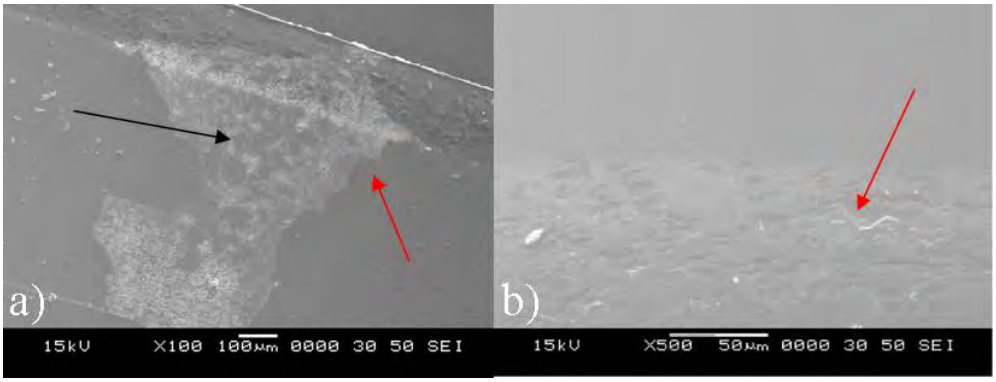

Figure 4. 24 SEM micrographs indicating edge corrosion on the OC50 sample after exposure to an acrylic acid concentration of 0.3, a) pre tensile testing b) post tensile testing. Black arrow indicates acidic corrosion, red arrows indicate cracking and delamination.

With regards to the samples that exhibited reduced critical onset strains, the SEM micrographs in Figure 4. 25 indicate that the corrosive spot formation may act as crack initiation sites and also result in greater crack propagation. They also show that acidic corrosion occurs in a non uniform manner across the sample. It can also be seen that cracking of the ITO layer is more prominent in samples that have been subjected acidic exposure, compared to the reference samples that were not exposed to any acrylic acid. This adds weight to the notion that when tested in tension, the exposure to acrylic acid reduces the ITO/PET systems ability to resist strain.

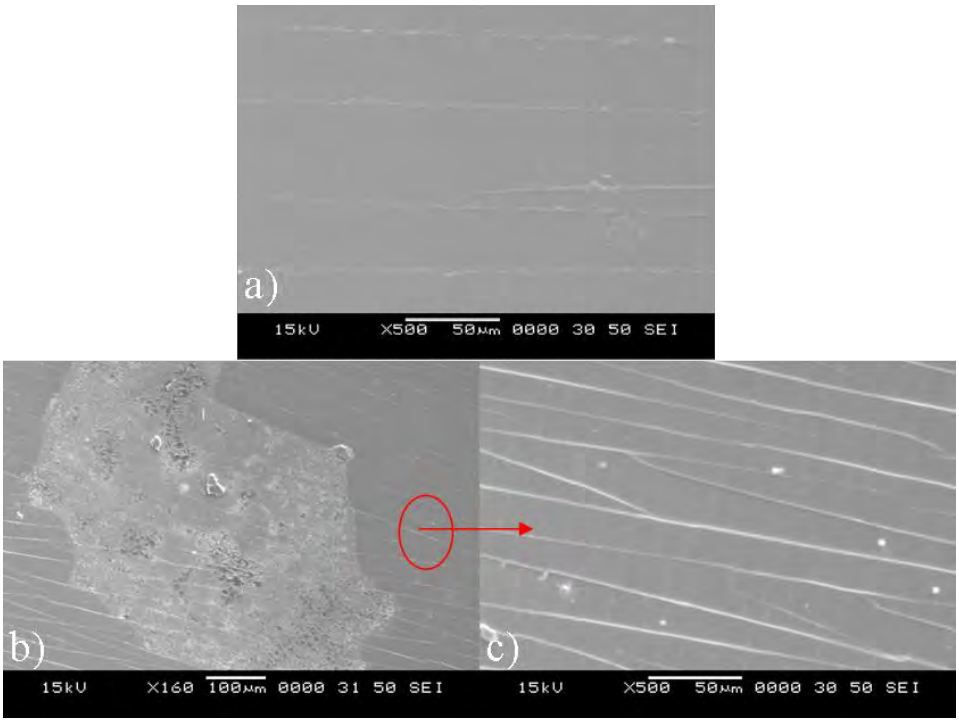

Figure 4. 25 SEM micrographs comparing the reference sample to a sample exposed to an acidic concentration of 0.3 M for two hours on the OC100 sample, a) no acid b) and c) 0.3 M acrylic acid.

4.3.3 Ex situ surface analysis after monotonic bending

Surface analysis of the ITO/PET systems after monotonic bending in both tension and compression were investigated using an *ex–situ* SEM technique.

Figure 4. 26 displays the surface of the OC100 sample after monotonic bending and exposure to acrylic acid. The sample was flexed to in tension to a radius of 4 mm radius of curvature. From this channelling cracks and delamination can be clearly seen via black and red arrows respectively. The crack formation in this experiment is consistent with the uniaxial tensile test, as the cracks are parallel to one another and are perpendicular to the load direction. It can also be seen that the acrylic acid corrosion sites are facilitating failure. Furthermore the micrographs indicate catastrophic delamination in a sample exposed to an acrylic acid concentration of 0.2 M, whilst this is not seen at the higher concentration of 0.5 M. This indicates that acrylic acid is not the primary failure mechanism, moreover it supports the indication that stress corrosion cracking as the primary failure mechanism when these ITO/PET systems are monotonically bent in tension.

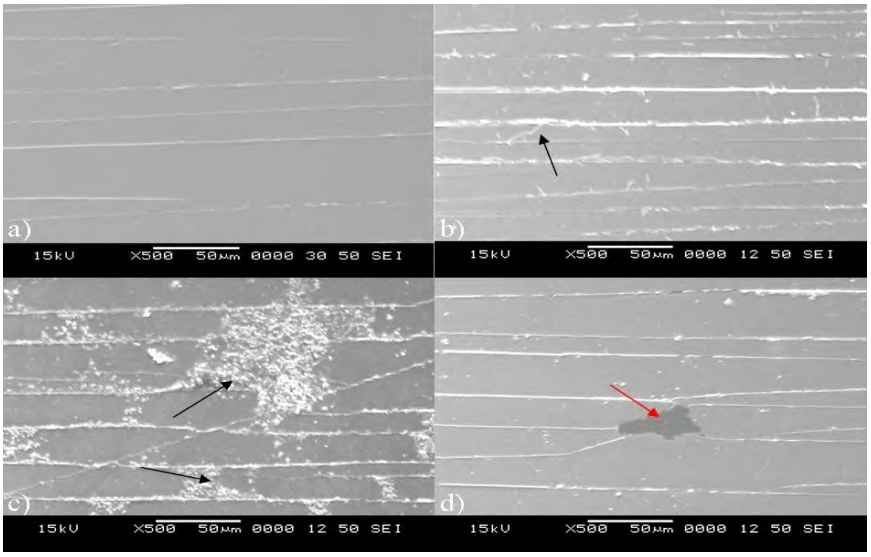

Figure 4. 26 SEM micrograph of the OC100 sample after monotonic bending in tension, a) no acid, b) 0.1 M, c) 0.5 M d) 0.2 M. Red arrow indicates catastrophic delamination, black arrows indicate cracking at corrosion sites.

Figure 4. 27 shows an SEM micrograph of the OC100 sample after monotonic bending under compression to a radius of curvature of 1mm. From these micrographs buckling delamination can be clearly seen. At some points over the sample, the buckled ITO film had actually detached from the substrate, resulting in a large gap formation between the ITO fragments. This delamination is the cause of the sharp increase in the increment of electrical resistance above the critical bending radius. It can also be seen that exposure to acrylic acid has not facilitated failure nor has it induced crack formation. This supports the claim that when an ITO/PET system is subjected to monotonic bending under compression, the failure mechanism is dependent upon the intrinsic properties of the ITO/PET system.

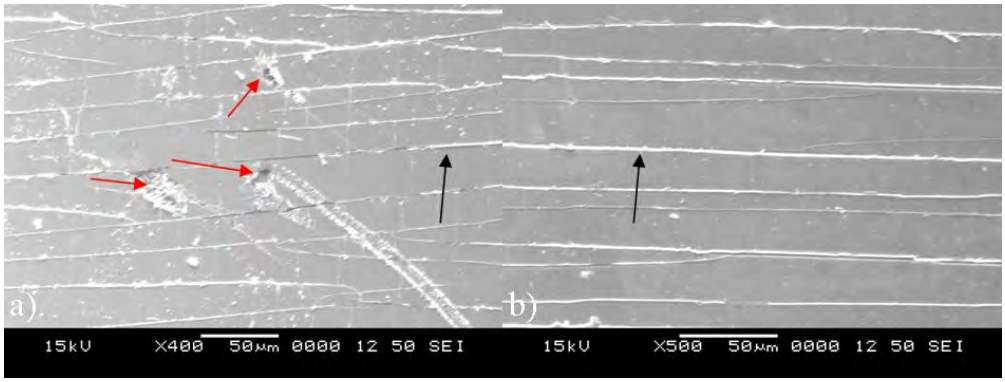

Figure 4. 27 SEM micrographs of OC100 sample after monotonic bending in compression, a) no acid b) 0.5 M. Black arrows indicate channelling cracks and red arrows indicate delamination.

At this point it should also be noted that the largest amount of damage for the ITO/PET systems tested in both tension and compression was seen in the middle of the sample. This region of damage is consistent with previous work (Park, 2004) where the stress that is induced through bending in either tension or compression is position dependent. This indicates that curvature created through bending is not uniform throughout its length, with the highest strains located at the centre of the sample.

4.3.4 Ex situ SEM observations of ITO/PET systems after High Frequency Reciprocating Rig wear test

The ITO coated films were investigated after tribological testing using the SEM technique combined with energy-dispersive X-ray spectroscopy in order investigate if any wear transfer had taken place. After *ex-situ* EDS, it can be confirmed that wear transfer from the PTFE ball to the ITO/PET system had taken place as a result of the HFRR wear test. Figure 4. 28 displays the wear scar where wear debris can be seen and Figure 4. 29 can statistically confirm the presence of fluorine at this targeted point.

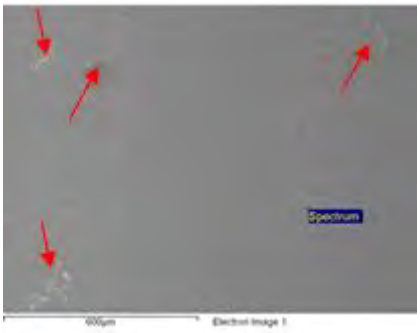

Figure 4. 28 SEM micrograph indicating wear transfer from PTFE ball. "Spectrum" indicates the site at which EDS had taken place, red arrows indicate wear debris.

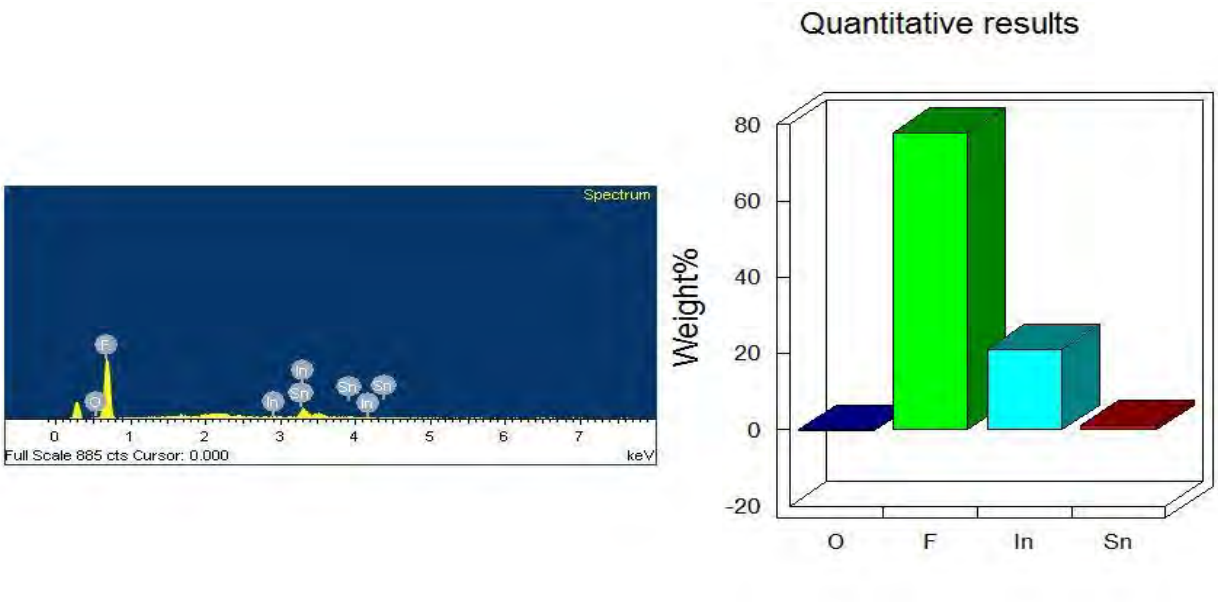

Figure 4. 29 Statistical confirmation of wear transfer via Inca EDS that Fluorine (F) Indium (In) Tin (Sn) and Oxygen (O) are present.

5. Conclusions

Through the work of this study the optical, electro-mechanical and tribological properties of commercial ITO/PET systems have been thoroughly investigated. It can be seen that whilst commercial ITO/PET systems can be viable candidates for flexible display technologies, great care and understanding of the systems properties must be taken into account during the design phase for their use in service and during the manufacturing process. From the work conducted in this study, the following conclusions can be made;

- When exposed to acrylic acid ITO/PET systems show an increase in optical transmission in the visible spectrum due to corrosion of the ITO layer. Furthermore as the concentration of acrylic acid is increased, the optical transmission also increases.
- The effect of acrylic acid exposure on the optical properties of these systems creates a major problem; as visual detection of failure would most likely not occur due to an increase in optical transmission, which may allow for harmful corrosion to go unnoticed.
- Even at low acidic concentrations such as 0.1 M a significant increase in electrical resistance could be seen for all samples. Furthermore an increase of over 100% shown at 0. 1M for the 300 Ω/□ sample. It was shown that by increasing the acidic concentration, the surface resistance will also increase. It was also noted that exposure to acrylic does not systematically affect the ITO/PET system, but rather causes apparently random damage throughout the ITO surface and the electrical properties of these commercial ITO/PET systems are dependent on the ITO layer thickness.
- Commercial 50 Ω/□, 100 Ω/□ and 300 Ω/□ samples displayed critical onset strains of 1.3%, 2.3% and 2.1% respectively.

- Exposure to acrylic acid prior to induced uniaxial strain results in a significant reduction of the samples ability to resist strain due to weakening of the ITO film as a result of stress corrosion cracking.
- During monotonic bending whilst the sample is under tensile stress, conductive failure occurs at around 5, 5.6 and 2.3 mm for the 50 Ω/□, 100 Ω/□ and 300 Ω/□ samples respectively. It was seen that ITO/PET systems with thin ITO layers display a greater degree of flexibility under tension than ITO/PET systems with a thick ITO layer. Thus it can be said that during monotonic bending under tensile stress, the mechanical properties of the ITO/PET systems are dependent on the ITO film thickness.
- Whilst subjected to bending in tension exposure to acrylic acid results in a significant increase in the critical onset radius, even at low concentrations such as 0.1 M. Although acidic corrosion was not seen to be the sole cause for failure, it does however facilitate failure. Therefore it can be seen that stress-corrosion cracking is the primary failure mechanism exhibited.
- Compared to the samples tested under tension, the ITO/PET systems examined under compressive loads show low critical radius of curvature values (in the vicinity of 2 mm for all samples). Post critical radius the increment of resistance sharply increases in the same manner as for the samples examined under tension. Results showed that unlike samples tested in tension, exposure to acrylic acid does not have any significant effect on the degree of flexibility for the ITO/PET systems examined in compression.
- Reciprocating wear was located in a centralised location; micrographs indicated that only the part of the sample subjected to wear exhibited crack formation and

propagation, resulting in the sample displaying affected and non affected regions. Critical failure was seen at around 500, 220 and 570 sliding cycles for the 50 Ω/□, 100 Ω/□ and 300 Ω/□ samples respectively.

- Exposure to acrylic acid resulted in the number of cycles to failure being reduced for all samples and increasing the concentration of acrylic acid was not seen to have a significant effect on the number of cycles to critical failure.
- *Ex situ* EDS of the wear scar confirmed that wear transfer had taken place.

To conclude; the exposure of acrylic acid has a significant detrimental effect on the ITO/PET systems ability resist strain under tensile loads, even at low concentrations such as 0.1M, it decreases the ITO/PET systems tribological properties and furthermore it corrodes the ITO layer which in turn increases the ITO/PET systems optical transmission. This increase in optical transmission can causes an area for concern as the detrimental effects of acrylic acid exposure may go un-noticed. However, acrylic acid exposure was not seen to cause any significant effect on the degree of flexibility of these ITO/PET systems when subjected to compressive strains.

6. Future work

Commercial ITO coated PET substrates were used within this investigation to display the effects of acrylic acid on their electro-mechanical behaviour. Future work is recommended on polymer substrates coated via other techniques such as pulsed laser deposition, sol gel processing or controlled magnetron sputtering. This would allow for full control over deposition parameters and give a greater range of ITO thicknesses.

Furthermore, depositing ITO on polymer substrates could also allow the deposition of buffer layers, such as aluminium oxide (Al_2O_3). This would allow for an investigation into their influence on the electro-mechanical properties of these thin film systems.

A range of polymer substrates could also be investigated in the future such as PEN or PC to allow a comparison against the ITO/PET system. Moreover, conductive polymers such as poly(3,4-ethylenedioxythiophene) doped with polystyrene sulfonic acid (PEDOT:PSS) have been discussed as possible candidates to replace ITO films for flexible displays and could be investigated in future studies.

Due to the high costs involved with manufacturing ITO layers, alternative TCO's such as zinc oxide (ZnO) could be used. Once these alternative TCO's have been effectively deposited onto a polymer substrate, results of opto-electrical and electro-mechanical tests can be compared with those for ITO/PET systems.

Tribo-corrosion of thin films for flexible displays has been investigated in this work. However, only dry sliding conditions were introduced. Future work is encouraged to include both dry and wet sliding conditions to develop further knowledge of the tribological properties of these thin films.

Finally, during acrylic acid exposure, any change in electrical resistance could be monitored in relation to time via in-situ electrical resistance measurements using appropriate beakers and π-shaped samples.

7. References

BEUTH JR, J. L. 1992. Cracking of thin bonded films in residual tension. *International Journal of Solids and Structures,* 29**,** 1657-1675.

BOUTEN, P. C. P. 2002. Failure test for brittle conductive layers on flexible display substrates. *EURODISPLAY***,** 313-316.

BOUTEN, P. C. P., SLIKKERVEER, P. J. & LETERRIER, Y. 2005. Mechanics of ITO on Plastic Substrates for Flexible Displays. *Flexible Flat Panel Displays.* John Wiley & Sons, Ltd.

CAIRNS D.R., P. D. C., CRAWFORD G.P. 2001. The Mechanical Reliability of Sputter-Coated Indium Tin Oxide Polyester Substrates for Flexible Display and Touchscreen Applications. *Society of Vacuum Coaters* 44th Anual Technical Conference Proceedings 856-5921.

CAIRNS, D. R., WITTE, R. P., SPARACIN, D. K., SACHSMAN, S. M., PAINE, D. C., CRAWFORD, G. P. & NEWTON, R. R. 2000. Strain-dependent electrical resistance of tin-doped indium oxide on polymer substrates. *Applied Physics Letters,* 76**,** 1425-1427.

CHEN, M., WANG, X., YU, Y. H., PEI, Z. L., BAI, X. D., SUN, C., HUANG, R. F. & WEN, L. S. 2000. X-ray photoelectron spectroscopy and auger electron spectroscopy studies of Al-doped ZnO films. *Applied Surface Science,* 158**,** 134-140.

CHEN, Z., COTTERELL, B. & WANG, W. 2002. The fracture of brittle thin films on compliant substrates in flexible displays. *Engineering Fracture Mechanics,* 69**,** 597-603.

CHEN, Z., COTTERELL, B., WANG, W., GUENTHER, E. & CHUA, S.-J. 2001a. A mechanical assessment of flexible optoelectronic devices. *Thin Solid Films,* 394**,** 201-205.

CHEN, Z., COTTERELL, B., WANG, W., GUENTHER, E. & CHUA, S. J. 2001b. A mechanical assessment of flexible optoelectronic devices. *Thin Solid Films,* 394**,** 202-206.

CHOI, K.-H., JEONG, J.-A., KANG, J.-W., KIM, D.-G., KIM, J. K., NA, S.-I., KIM, D.-Y., KIM, S.-S. & KIM, H.-K. 2009. Characteristics of flexible indium tin oxide electrode grown by continuous roll-to-roll sputtering process for flexible organic solar cells. *Solar Energy Materials and Solar Cells,* 93**,** 1248-1255.

CHOI, M.-C., KIM, Y. & HA, C.-S. 2008. Polymers for flexible displays: From material selection to device applications. *Progress in Polymer Science,* 33**,** 581-630.

CHUNG, W., THOMPSON, M. O., WICKBOLDT, P., TOET, D. & CAREY, P. G. 2004. Room temperature indium tin oxide by XeCl excimer laser annealing for flexible display. *Thin Solid Films,* 460**,** 291-294.

CRAWFORD, D. R. C. A. G. P. C. D. R. C. A. G. P. 2000. wear resistance of indium tin oxide coatings on polyethylene terephthalate substrates for touch screen applications. *Society for Information Display 2000 Digest***,** 1-4.

CRAWFORD, G. P. 2005. *Flexible flat panel display technology,* New York Wiley

FAN, J. C. C. & GOODENOUGH, J. B. 1977. Xray photoemission spectroscopy studies of Sn doped indium oxide films. *Journal of Applied Physics,* 48**,** 3524-3531.

FISCHER-CRIPPS, A. C. 1999. The Hertzian contact surface. *Journal of Materials Science,* 34**,** 129-137.

GUTIERREZ, M. P., LI, HAIYONG., PATTON, JEFFREY. 2002. Thin Film Surface Resistivity. *Experimental Methods in Materials Engineering.*

HAO, L., DIAO, X., XU, H., GU, B. & WANG, T. 2008. Thickness dependence of structural, electrical and optical properties of indium tin oxide (ITO) films deposited on PET substrates. *Applied Surface Science,* 254**,** 3504-3508.

HERTZ, H. 1896. *Miscellaneous papers by Heinrich Hertz ... with an introduction by Philipp Leonard ; authorised English translation by D.E. Jones ... and G.A. Schott,* London, Macmillan.

HUTCHINSON, J. W. 1996. Mechanics of thin films and multilayers: Course Notes *Technical Report* Denmark Technical University of Denmark

KIM, H. 2007 Transparent Conducting Oxide Films *Pulsed Laser Deposition of Thin Films: Applications-Led Growth of Functional Materials.* Hoboken, New Jersey Wiley & Sons, inc. .

KIM, H., HORWITZ, J. S., KUSHTO, G. P., KAFAFI, Z. H. & CHRISEY, D. B. 2001. Indium tin oxide thin films grown on flexible plastic substrates by pulsed-laser deposition for organic light-emitting diodes. *Applied Physics Letters,* 79**,** 284-286.

LAKES, R. 1987. Foam Structures with a Negative Poisson's Ratio. *Science,* 235**,** 1038-1040.

LAN, Y. F., PENG, W. C., LO, Y. H. & HE, J. L. 2009. Indium tin oxide films deposited by thermionic-enhanced DC magnetron sputtering on unheated polyethylene terephthalate polymer substrate. *Materials Research Bulletin,* 44**,** 1760-1764.

LAN, Y. F., PENG, W. C., LO, Y. H. & HE, J. L. 2010. Durability under mechanical bending of the indium tin oxide films deposited on polymer substrate by thermionically enhanced sputtering. *Organic Electronics,* 11**,** 670-676.

LETERRIER, Y., BOOGH, L., ANDERSONS, J. & MÅNSON, J. A. E. 1997. Adhesion of silicon oxide layers on poly(ethylene terephthalate). I: Effect of substrate properties on coating's fragmentation process. *Journal of Polymer Science Part B: Polymer Physics,* 35**,** 1449-1461.

LETERRIER, Y., FISCHER , C., MEDICO , L., DEMARCO , F., MANSON , J.-A. E., BOUTEN , P., DEGOEDE , J. & NAIRN , J. A. 2003 Mechanical Properties of Transparent Functional Thin Films for Flexible Displays. *46th Annual Technical Conference Proceedings of the Society of Vacuum Coaters***,** 1-6.

MACDONALD, W. A. 2004. Engineered films for display technologies. *Journal of Materials Chemistry,* 14**,** 4-10.

MORRIS, N. J., SIERROS, K. A., RAMJI, K., CAIRNS, D. R., KUKUREKA, S. N. & SID 2008. Mechanical assisted corrosion: An investigation of thin film components used in flexible optoelectronic applications. *2008 Sid International Symposium, Digest of Technical Papers, Vol Xxxix, Books I-Iii.*

PAINE, D. C., YEOM, H.-Y. & YAGLIOGLU, B. 2005. Transparent Conducting Oxide Materials and Technology. *Flexible Flat Panel Displays.* John Wiley & Sons, Ltd.

PARK, J.-B., HWANG, J.-Y., SEO, D.-S., PARK, S.-K., MOON, D.-G. & HAN, J.-I. 2004. Position Dependent Stress Distribution of Indium-Tin-Oxide on Polymer Substrate by Applying External Bending Force. *The Japan Society of Applied Physics,* 43 2677-2680.

POPOV, V. L. 2010. *Contact Mechanics and Friction Physical Principles and Applications,* Berlin, Springer.

POTOCZNY, G. A. 2011. *Electro-Mechanical Behaviour of Indium Tin Oxide Coated Polymer Substrates for Flexible Electronics* Doctor of Philosophy PHD, University of Birmingham

RUNYAN, W. R. & SHAFFNER, T. J. 1997. *Semiconductor measurements and instrumentation,* New York ; London, McGraw-Hill.

SHIN, H. S., KOO, J. B., JEONG, J. K., MO, Y. G., CHUNG, H. K., CHEON, J. H., CHOI, J. H. 2005. 4.1 inch Top-Emission AMOLED on Flexible Metal Foil. *SID Symposium Digest of Technical Papers,* 49**,** 1642-1645.

SIERROS, K. A. 2006. *Mechanical properties and characterisation of substrates for flexible displays* Doctor of Philosophy University of Birmingham

SIERROS, K. A., BEJITUAL, T. S., CRONIN, S., KESSMAN, A. J., KUKUREKA, S. N. & CAIRNS, D. R. 2011. Tribo-corrosion of Ag and Ag-alloy ITO multilayers used in solar energy applications. *Wear,* 271**,** 1438-1444.

SIERROS, K. A., MORRIS, N. J., KUKUREKA, S. N. & CAIRNS, D. R. 2009a. Dry and wet sliding wear of ITO-coated PET components used in flexible optoelectronic applications. *Wear,* 267**,** 625-631.

SIERROS, K. A., MORRIS, N. J., RAMJI, K. & CAIRNS, D. R. 2009b. Stress-corrosion cracking of indium tin oxide coated polyethylene terephthalate for flexible optoelectronic devices. *Thin Solid Films,* 517**,** 2590-2595.

SLIKKERVEER, P. J. Bending the display rules: Options and Challenges for Flexible Displays. Eurodisplay 2002 Nice. 273 - 276.

WANG, J. S., SUGIMURA, Y., EVANS, A. G. & TREDWAY, W. K. 1998. The mechanical performance of DLC films on steel substrates. *Thin Solid Films,* 325**,** 163-174.

WEBER A, D. S., PLICHTA A, HABECK A. 2002. Thin glass-polymer systems as flexible substrates for displays. *Society for Information Display 2002 International Symposium,* 33**,** 53-55.

YOUNG-SOON KIM, Y.-C. P., S.G. ANSARI, JEONG-YOUNG LEE, BYUNG-SOO LEE, & SHIN, H.-S. 2003. Influence of O2 admixture and sputtering pressure on the properties of ITO thin films deposited on PET substrate using RF reactive magnetron sputtering. *Surface and Coatings Technology***,** 229-308.

Z. SUOA, E. Y. M., H. GLESKOVA, AND S. WAGNER 1999. Mechanics of rollable and foldable film-on-foil electronics. *American Institute of Physics,* 74**,** 1177 - 1179.